UNIVERSITY OF CALGARY

Characterisation Of The Composition And The Dynamic Properties Of PML Nuclear Bodies

By

François-Michel Boisvert

A THESIS SUBMITTED TO THE FACULTY OF GRADUATE STUDIES IN PARTIAL FULFILLMENT OF THE REQUIREMENTS FOR THE DEGREE OF MASTER OF SCIENCE

DEPARTMENT OF BIOCHEMISTRY AND MOLECULAR BIOLOGY

CALGARY, ALBERTA

NOVEMBER, 2000

Abstract

The promyelocytic leukemia (PML) nuclear body is found in every cell. Despite its obvious links to oncogenesis and viral infection, the cellular role of this subnuclear domain remains unclear. I have demonstrated that the PML nuclear body is a protein based structure surrounded by nascent RNA and highly acetylated chromatin. Moreover, I have shown, using fluorescence recovery after photobleaching, that CBP moves rapidly into and out of PML bodies. In contrast, Pml and Sp100 are relatively immobile in the nucleoplasm and within PML nuclear bodies. They possess the characteristics expected of proteins that would play a structural role in the integrity of these sub-nuclear domains and would be responsible for concentrating other functional proteins such as CBP. My results support the model in which the PML nuclear body is responsible for the formation of a transcriptionally active environment that may be specific to a small subset of genes.

Acknowledgements

My supervisor, Dr. David P. Bazett-Jones

My Committee members and examiners, Dr. R.N. Johnston, Dr. S. Lees-Miller, and Dr. B. Burke, and Dr. A Kossakowska for their counseling and support.

All the member of the lab; Mike Kruhlak, Priscilla Hill, Manfred Herfort, Ying Ren, Dr. Michael Schoel, Maryse Fillion, Dr. Michael Hendzel, Alan Box and Lesley Marshall.

Mes parents, Louise et Georges Boisvert pour m'avoir poussé à poursuiver mes études.

My parents-in-Law, Lise and Doug Scott, for dragging me to the Wild West.

My fiancée, Michelle, for her support, love and understanding.

My two cats, Bretelle and Trouser, for behaving so badly.

And all my friends, for gladly accepting to drink beer with me every Friday.

Dedicated to my future wife, Michelle Scott, for her support, understanding and devotion throughout my education.

Table of Contents

List of Tables

List of Figures and Illustrations

List of Symbols, Abbreviations, Nomenclature

μg	microgram
μL	microliter
μM	micromolar
°C	degree Celsius
5-FU	5-fluorouridine
Ad5	Adenovirus-5
APL	Acute promyelocytic leukaemia
APS	Ammonium persulfate
ATCC	American type culture collection
ATP	adenosine 5'-triphosphate
ATRA	All-trans retinoic acid
BLM	Bloom syndrome protein
BRCA	Breast cancer susceptibility gene product
BrdU	bromo-deoxy-uridine
CBP	CREB binding protein
CCD	Cooled coupled detector

cDNA	Cloned (recombinant) DNA
CHO	Chinese hamster ovary
CREB	Cyclic-AMP response element binding protein
CTAB	Cetyl-trimethyl amonium bromide
DAPI	4'-6-diamidino-2-phenylindole
DIC	Differential interference contrast
DMEM	Dubelcco's modification of Eagle's minimal essential medium
DMP-30	2,4,6-Tri(dimethylaminomethyl)phenol
DMSO	Dimethylsulfoxide
DNA	Deoxyribonucleic acid
dNTP	2'-deoxynucleotide 5'-triphosphate
DRB	5,6-dichloro-β-D-ribofuranosylbenzimidazole
DTT	dithiothreitol
EDTA	Ethylynediamine-tetraacetic acid
EIF-4E	Eukaryotic translation initiation factor 4E
ESI	Electron spectroscopic imaging
eV	Electron volts

FBS	Fetal bovine serum
FLIP	Fluorescence loss in photobleaching
FRAP	Fluorescence recovery after photobleaching
FU	5 - Fluorouridine
g	gram
GFP	Green fluorescent protein
GR	Glucocorticoid receptor
HA	Hemagglutinin A
HAT	histone acetyltransferase
HAUSP	Herpesvirus associated ubiquitin-specific protease
HDAC	histone deacetylase
HIV	Human Immunodeficiency Virus
HSV	Herpes simplex virus
HTLV	Human T-cell leukemia virus
IGC	Interchromatin granule cluster
JMEM	Joklik's minimal essential medium
JNK	Jun N-terminal kinase

kb	kilobase pair
kDa	kilodalton
LB	Luria-Bertani bacterial medium
LMP-2, -7	Low molecular weight protein of the proteasome complex
M	molar
MDM2	Mouse double minute protein
mg	milligram
MHC	Major histocompatibility complex
mL	milliliter
mM	millimolar
MMTV	Mouse mammary tumor virus
mRNA	messenger RNA
NaCl	sodium chloride
NDP	Nuclear Domain Protein
ng	nanogram
NMA	Nadic methyl anhydride
NPM	Nucleophosmin

NSA	Nonenyl succinic anhydride
NuMa	Nuclear mitotic apparatus protein
O.D.	optical density
PBC	Primary biliary cirrhosis
PBS	Phosphate buffered saline
PIC1	PML interacting clone 1
PKA	Protein kinase A
PLZF	Promyelocytic leukaemia zinc finger protein
PML	Promyelocytic leukaemia
RAD51/52	Response to alkylation damage proteins
RanGAP1	Ran GTPase-activating protein 1
RAR	Retinoic Acid Receptor
Rb	Retinoblastoma tumor suppressor protein
RBCC	RING B-Boxes Coiled-Coil Domain
RNA	Ribonucleic acid
rpm	Revolutions per minute
SDS	Sodium dodecylsulphate

SDS-PAGE	SDS polyacrylamide gel electrophoresis
SUMO1	Small ubiquitin-like modifiers 1
SV40	simian virus 40
TAE	Tris-acetate EDTA buffer
TAP-1, -2	Transporter associated with antigen processing proteins
TBST	TRIS buffer saline triton X-100
TEMED	N,N,N',N'-tetramethylethyldiamine
TFII	Transcription factor for RNA polymerase II
TIF1	Transcriptional intermediary factors 1
TRAF2	(TNF-alpha) receptor-associated factor 2
TRIS	Tris(Hydroxymethyl)Aminomethane Hydrochloride
UTP	Uridine triphosphate

Introduction

Overview

The cell nucleus is highly organized and divided into well-defined sub-domains. In contrast to cytoplasmic organelles, the different sub-nuclear compartments are not separated from the surrounding by a lipid bilayer. Instead, these structures are defined by a concentration of specific proteins within a defined area that retain a typical size, shape and number depending on protein function. It is not known how such compartments are formed and it remains to be shown if an underlying structural framework participates in a regulated assembly fashion or whether they are simply a confined local concentration of factors. It has been recently shown that different proteins of such nuclear compartments have a rapid rate of association-dissociation between the nucleoplasm and their nuclear compartment (Phair & Misteli, 2000). However, such studies do not demonstrate how these very mobile proteins are concentrated within a defined region.

The PML gene encodes a tumour suppressor protein associated with a distinct subnuclear domain, the PML nuclear body. The cellular role of the PML-containing nuclear bodies remains elusive despite links to oncogenesis and viral replication.

Discovery of PML Nuclear Bodies

More than 15 years ago, patients with primary biliary cirrhoris were shown to have autoantibodies recognizing so-called nuclear dots (Bernstein *et al.*, 1984). Primary Biliary Cirrhosis (PBC) is an autoimmune liver disease beginning with the destruction of the bile ducts and ending in a complete cirrhoris of the liver. Use of sera from these patients led to the discovery and cloning of the first biochemical component of PML nuclear bodies, Sp100 (Szostecki *et al.*, 1990). Approximately 30% of the patients with PBC have antibodies that are highly specific to Sp100.

Other proteins, such as PML, have also been shown to be the target of autoantibodies within patients with PBC (Sterndorf *et al.*, 1995). Autoantibodies against both Sp100 and PML often co-occur in sera of patients with PBC (Sterndorf et al., 1995). This co-occurrence of antibodies recognizing proteins present in the same multi-protein complex or structure may indicate that intact PML nuclear bodies complexes are released from destroyed cells during PBC and that they are the initial target for autoimmunization.

PML Nuclear Bodies Are Discrete Nuclear Structures

The nucleus is highly compartmentalized into organized structural and functional domains. Many of those subnuclear domains have been associated with a particular biochemical function. For example, nucleoli are sites of ribosomal RNA synthesis, processing and assembly into ribosomes (Scheer & Weisenberger, 1994). Interchromatin granule clusters, or IGCs, have been shown to be enriched in splicing factors and are likely to be involved in post-transcriptional modifications (Wei *et al.*, 1999). The PML nuclear body is a nuclear matrix-associated structure of 250-500 nm in diameter that is present in the nucleus of almost every cell line (Ascoli & Maul, 1991; Chang *et al.*, 1995; De Graaf *et al.*, 1992; Grande *et al.*, 1996; Stuurman *et al.*, 1992). There are approximately ten of these structures per nucleus, though this can vary considerably depending on the cell type, cell cycle and other factors (Ascoli & Maul, 1991). Electron microscopic analysis has revealed that the PML nuclear body is spherical shaped (De Graaf et al., 1992; Hodges *et al.*, 1998; Stuurman et al., 1992). Multiple different biological and biochemical functions have been attributed to the PML nuclear bodies. However, the cellular role of the PML nuclear body remains uncertain, despite its obvious link to oncogenesis, viral infection and transcription (Slack & Gallagher, 1999; Sterndorf *et al.*, 1997a).

Nuclear Architecture

The presence of an organizing principal within the cell nucleus that is analagous to the cytoskeleton has been hotly contested over the years. Recently, it has become practical to study directly the dynamics and motion of chromatin and nonchromatin elements of the cell nucleus. Consequently, in the absence of a convincing demonstration of a nuclear skeleton within unfractionated nuclei, it is possible to determine whether biomolecules behave as if they are embedded in an organizing supramolecular structure or whether they are subject to substantial Brownian motion. The results of such studies are compelling. Chromatin (Abney *et al.*, 1997; Kanda *et al.*, 1998; Marshall *et al.*, 1997) and nonchromatin structures such as nuclear speckles (Misteli *et al.*, 1997) and foci enriched in transcription factors are constrained from substantial Brownian motion, strongly supporting the view that there is a component or components of the cell nucleus that function to restrict the mobility of macromolecular complexes within the cell nucleus.

The cell nucleus has a number of compositionally distinct domains (Schul *et al.*, 1998). This implies a mechanism for organizing biochemical components into discrete supramolecular structures. An example is the nonchromatin extranucleolar structure of the cell nucleus called the interchromatin granule cluster (IGC). This structure is more widely known by the nuclear speckles that are observed by indirect immunofluorescence when cells are stained with antibodies recognizing small nuclear ribonuclear proteins (RNPs) or SC-35 (for review, see (Spector *et al.*, 1993)). The well-defined boundaries of nuclear speckles, when imaged by indirect immunofluorescence, indicate that they are discrete nuclear structures. Their large dimensions indicate that a physical continuity is maintained over relatively long distances. However, when these structures are imaged by standard electron microscopy, they appear as clusters of discrete 20- to 25-nm ribonucleoprotein particles. The question that arises is, what is the basis is for the cluster integrity? Since this structure does not contain any DNA, the organization of the

ribonucleoproteins must depend on protein-protein interaction with an underlying organizing structure rather then protein-DNA interaction. In another example, transcriptional regulators exist in many hundred smaller nuclear foci that occur both in association and away from chromatin (Grande et al., 1996; Hendzel *et al.*, 1998). It is compelling to invoke the presence of a protein architecture to organize these factors into the domains observed in both fixed (Grande *et al.*, 1997; van Steensel *et al.*, 1995) and unfixed cells (Fejes-Toth *et al.*, 1998; Misteli et al., 1997; Sleeman *et al.*, 1998). Moreover, these factors are found to be insoluble in nuclei where the DNA has been removed by digestion with DNAse I. Splicing snRNPs have a complex steady-state localisation within the nucleus. The result of the association of snRNPs with several distinct subnuclear structures such as IGCs, coiled bodies and nucleoli, in addition to a diffuse nucleoplasmic compartment, indicate they are required at multiple sites within the nucleus (Sleeman & Lamond, 1999). The reasons for snRNP accumulation in these different structures are unclear. However, the absence of DNA in most of these structures indicates that an organizing structure must be responsible for creating such environment. PML nuclear bodies are another example of such a structure that is devoid of DNA but can still concentrate specific proteins in a defined region (Zhong *et al.*, 2000a).

A nucleus that spatially organizes biomolecules through specialization on an underlying architecture may be fundamentally different in the mechanisms that serve to transcribe, replicate, and repair DNA, process and export RNA, and transduce signals from that of a nucleus that is not ordered beyond the folding of chromatin. Consequently, it is essential to define and characterize such an architecture if one exists. The prospect that a definable protein architecture exists in the cell nucleus was first brought to light by biochemical fractionation experiments pioneered by Berezney and Coffey (1974, 1977). The original preparation used 2 M NaCl and nuclease digestion to extract a DNA-based structure. Berezney and Coffey introduced the term "nuclear matrix" to refer to this high-salt, DNase-resistant fraction of the cell nucleus. Despite the absence of

direct evidence that these procedures generate nuclear structure through a precipitation of soluble nuclear components, experiments involving the isolation of nuclear structures have often been dismissed on this basis. In the face of mounting skepticism, methods involving radically different isolation procedures were developed (for review, see (Martelli *et al.*, 1996)) and, perhaps surprisingly, were found to generate nuclear remnants with similar morphological properties to the original preparation of Berezney and Coffey (1974, 1977). The most elegant procedure involves encapsulating cells in agarose and digesting the chromatin with restriction endonucleases, followed by electroeluting the chromatin in "physiological buffers" (Jackson & Cook, 1985). This isolation procedure enables the visualization within the interchromatin space of an intermediate filament-like protein network, which closely resembles preparations by more harsh salt extraction procedures (Jackson *et al.*, 1988).

If a network of protein and/or RNA is present in the cell nucleus, as supported by the extensive nuclear matrix literature, it is essential to develop an approach that is capable of ultrastructural analysis without disrupting individual components of the cell nucleus. This is particularly true for chromatin, which is the principal basis for the existence of the cell nucleus as a separate cellular compartment. To this end, we have been applying and optimizing an analytical microscopic technique for the study of nuclear components. Electron spectroscopic imaging (ESI) couples a conventional transmission electron microscope with an analytical imaging spectrometer. The technique is analogous to the resolution of different energies of light to extract compositional information (e.g., fluorescence microscopy) in light microscopy. The separation of electrons that vary in energy after interacting with a specimen can be exploited to extract compositional information from the electron microscope. Detailed descriptions of the applications of this method to the study of the structure and composition of the cell nucleus have been presented previously (Bazett-Jones & Hendzel, 1999; Bazett-Jones *et al.*, 1999; Hendzel & Bazett-Jones, 1996). Using ESI. we have established that it is

possible to resolve nucleic acids in nucleoprotein complexes and to quantify their mass and nucleic acid contents. This is achieved by imaging with electrons that have lost characteristic amounts of energy through interactions with phosphorus and nitrogen atoms of the specimen.

Using a fixation method identical to the preparations most commonly used for indirect immunofluorescent analysis of nuclear organization, it was shown that the interchromatin space, including IGCs, is rich in complexes that are composed predominantly of protein. A structural role for this protein component is most strongly indicated within IGCs, where the granules are embedded and linked together by a protein-based architecture. This indicates that there is a structural component of the cell nucleus in standard cytological preparations and in the absence of viral infection or nuclear fractionation.

Protein Components of PML Nuclear Bodies

Sp100

The Sp100 protein was the first biochemical component to be identified and cloned (Szostecki et al., 1990). Sp100 is a very acidic protein of PML nuclear bodies with a calculated molecular weight of around 53 kDa and shows an aberrant electrophoretic mobility of approximately 100 kDa on a SDS-PAGE gel (Szostecki et al., 1990). A number of transcripts resulting from alternative splicing have been identified and shown to encode a total of three proteins which differ in the C-terminal region: Sp100, Sp100B and SpAlt (Xie *et al.*, 1993). Sp100 is tightly bound to the nuclear matrix (Xie et al., 1993), although a small proportion is also present in the soluble fraction (nucleoplasm) after cellular fractionation (Szostecki *et al.*, 1987). The Sp100 shows several interesting sequence motifs. At the N-terminus of Sp100, there is a motif that is very similar to the peptide binding groove of MHC class I molecules (Sterndorf et al., 1997a). Expression of Sp100 fragments fused to a DNA binding domain has shown that a transcriptional activation domain is

located in the central region of the protein (Xie et al., 1993). This domain is very similar to the transactivating domain of viral proteins, such as HIV-1 Nef protein (Szostecki et al., 1990). However, Sp100 protein has also been shown to have transcription repression activity (Guldner *et al.*, 1992).

PML

The interest in PML nuclear bodies strongly increased when a protein involved in the development of Acute Promyelocytic Leukemia (APL), PML protein, was found to co-localize exactly with Sp100 (Ascoli & Maul, 1991; Dyck *et al.*, 1994; Szostecki et al., 1990). This protein was originally discovered in patients suffering from APL where the PML encoding gene was found to be translocated with the retinoic acid receptor alpha (RAR) gene (Borrow *et al.*, 1990; de The *et al.*, 1990; Kakizuka *et al.*, 1991). Expression of this fusion protein is sufficient for transformation of cells and induction of leukemias (Altabef *et al.*, 1996).

Different motifs have been found in the PML protein. The most interesting is a repeat of three cysteine-rich metal binding domains, that probably complex zinc, found at the N-terminus of the protein. This domain is called a RING finger and is shared by many proteins, including proto-oncogenes like the breast cancer susceptibility gene product BRCA1, the mouse double minute protein MDM2 or c-Cbl, as well as components of signal transduction pathways such as TRAF2 in the TNF pathway and CRAF1 in CD40 pathway (Slack & Gallagher, 1999; Sterndorf et al., 1997a). The RING finger has been shown to be essential for proper localization of PML protein to the PML nuclear bodies (Lai & Borden, 2000). Moreover, the overexpression of a PML protein containing a point mutation in the RING finger causes a disruption of the existing PML nuclear bodies (Borden, 2000). In addition to its RING finger, PML contains two B-Boxes, which are also zinc binding motifs (Borden *et al.*, 1996). This motif is followed by a coiled-coil domain, which mediates dimerisation/multimerisation of the protein (Kastner *et al.*,

1992; Perez *et al.*, 1993). This RING-B-Box-Coiled-Coil (RBCC) pattern is commonly found in a subgroup of RING finger proteins, including BRCA1, TIF1 and Rfp (Sterndorf et al., 1997a). The coiled-coil domain is followed by a serine-rich domain, which is thought to mediate transcription regulation activity (de The *et al.*, 1991; Fagioli *et al.*, 1998; Kakizuka et al., 1991).

A large number of alternatively spliced variants of PML have been identified. There are a total of 16 different proteins ranging from 47 kDa to 160 kDa in size (Fagioli *et al.*, 1992). Moreover, PML can be modified on three different sites by the small ubiquitin-like protein PIC1/SUMO1 (Duprez *et al.*, 1999; Muller *et al.*, 1998), each modification adding approximately 20 kDa to the protein. This means that the possible number of proteins of different size could reach as many as 4096! Some differences in the array of PML mRNA isoforms were observed in granulocytes and monocytes following interferon treatment, suggesting specific functions for some isoforms (Nason-Burchenal *et al.*, 1996). Despite the co-localization within PML nuclear bodies by immunofluorescence, PML and Sp100 proteins do not interact directly (Koken *et al.*, 1994; Sterndorf et al., 1995).

CBP

The co-activator CBP (CREB Binding Protein) has been found to localize in PML nuclear bodies (Boisvert *et al.*, 2000; LaMorte *et al.*, 1998). However, this is seen only when cells are labeled with an antibody recognizing the N-terminus of the protein (LaMorte et al., 1998). This protein has been first described as a factor binding to protein kinase A (PKA)-phosphorylated forms of CREB protein (Cyclic AMP Response Element Binding protein), which enhances transcription (Arany *et al.*, 1995; Kwok *et al.*, 1994). CBP is found complexed in a variety of DNA binding transcription factors, as well as with the RNA polymerase II holoenzyme itself (Giordano & Avantaggiati, 1999). CBP has also been shown to be a tumor suppressor, inhibiting cell growth when overexpressed and mutated in some

human tumors (Giordano & Avantaggiati, 1999). It has recently been shown that CBP has intrinsic acetyltransferase activity that can not only acetylate histone tails, but also other proteins, such as p53, TFIIE, TFIIH and many other proteins (Imhof *et al.*, 1997; Martinez-Balbas *et al.*, 1998; Ogryzko *et al.*, 1996). However, the transcription activation of CBP does not depend only on its ability to acetylate histone tails. There is an independent transcription activating domain (Giordano & Avantaggiati, 1999).

SUMO1/PIC1

SUMO1, Small Ubiquitin-like Modifier, (or PIC1, Sentrin, UBL1, GMP1) is a novel ubiquitin-like protein that was originally found to specifically interact with PML protein (Boddy *et al.*, 1996). Subsequently, SUMO1 was cloned independently by several other groups and found to interact with a variety of functionally distinct proteins, including the death domains of Fas/Apo-1, RAD51/52 and RanGAP1 (Duprez et al., 1999). Similar to ubiquitin, SUMO1 has been shown to covalently modify a number of target proteins, the best-characterised of which is RanGAP1. The modification does not lead to degradation, unlike ubiquitin, but targets RanGAP1 specifically to the nuclear pore complex (Matunis *et al.*, 1996). Modification occurs on a lysine of the target protein. In the case of PML nuclear bodies, both PML and Sp100 protein have been shown to be covalently modified by SUMO1 (Muller et al., 1998; Sterndorf *et al.*, 1997b). The exact role of this post-translational modification is still unclear, but it seems that modification of PML protein by SUMO1 is necessary for its localization within the PML nuclear bodies. However, modification of Sp100 is not necessary for proper targeting of this protein (Duprez et al., 1999).

Other Proteins

Several other components of the PML nuclear body have been identified.

I) NDP52 (nuclear dot protein of molecular weight of 52 kDa) was identified by immunoscreening of an expression library using an antibody that did not recognize Sp100 or PML from a patient with PBC (Sterndorf et al., 1995). It is predicted to contain a coiled-coil region and a cysteine-histidine rich region. No function has been attributed to this protein so far.

II) Two other proteins have been found using sera from PBC patients: NDP53 and NDP55 (Sterndorf et al., 1997a). However, the corresponding cDNAs have never been cloned.

III) HAUSP is a novel protease of the ubiquitin-specific family. It has been found to be responsible for reversing the SUMO1 modification (Everett *et al.*, 1997). It interacts with the HSV early protein Vmw110, which localizes to PML nuclear bodies during early viral infection (Everett et al., 1997). This protein is responsible for disrupting the PML nuclear bodies at a later stage of infection (Ishov & Maul, 1996). It is thought that recruitment of HAUSP to the PML nuclear bodies can reverse the equilibrium of SUMO1 modification of PML, which is necessary for the formation of PML nuclear bodies (Everett et al., 1997; Muller et al., 1998).

IV) BLM (Bloom Syndrome Protein) is also a constituent of the PML nuclear bodies and PML is required for its accumulation in these nuclear domains and for the normal function of BLM (Zhong *et al.*, 1999).

V) INT-6 has been characterized in the context of studies on the Tax protein of HTLV (Human T-Cell Leukemia Virus) (Desbois *et al.*, 1996). The gene encoding this protein was originally discovered as

one of the integration sites for the MMTV (Murine Mammary Tumor Virus). It has a predicted coiled-coil domain and was found to localize to PML nuclear bodies (Sterndorf et al., 1997a).

VI) The translation initiation factor eIF-4E was shown to partially overlap with PML nuclear bodies when PML was overexpressed. It was shown that PML could prevent the exportation of eIF-4E from the nucleus to the cytoplasm, where it acts as a transporter for some mRNA, such as Cyclin D1 mRNA (Lai & Borden, 2000).

VII) PML colocalizes with the nonphosphorylated fraction of the retinoblastoma protein (pRB) within nuclear bodies (Alcalay *et al.*, 1998). PML forms complexes with the nonphosphorylated form of pRB in vivo, and interacts with the pocket region of pRB (Alcalay et al., 1998). Functionally, PML abolishes activation of glucocorticoid receptor-regulated transcription by pRB (Alcalay et al., 1998; Zhong et al., 2000a).

VIII) Daxx was first identified as a protein that binds the cytosolic domain of Fas and links this receptor to an apoptosis pathway involving activation of Jun N-terminal kinase (JNK). Daxx is found in the nucleus where it localizes to PML nuclear bodies when PML is overexpressed, or when PML is heavily modified by SUMO1 (Ishov *et al.*, 1999; Torii *et al.*, 1999). Daxx seems to cooperate with PML to induce apoptosis using a novel pathway (Zhong *et al.*, 2000b).

IX) The p53 protein was briefly mentioned as being a component of PML nuclear bodies in a review, but as unpublished observations. It was also mentioned that it is interacting directly with PML protein (Zhong et al., 2000a).

PML Nuclear Bodies Role in Leukemia

Elucidation of the molecular biology of acute promyelocytic leukemia, or APL, represents a most successful translational research endeavour. The finding of how this particular form of cancer develops at the genetic and molecular level led to finding cures that are now successful with a rate of up to 75%. The defining molecular aberration in APL is the translocation of the gene coding for the alpha-receptor for retinoic acid gene, RARα, with one of four partner genes identified so far (Slack & Gallagher, 1999). Even though these fusion proteins lack classic transforming activity, they still have the ability to disrupt hematopoiesis by preventing promyelocytic maturation.

The first identified reciprocal translocation causing APL was between chromosomes 15 and 17 (Rowley *et al.*, 1977). The finding that retinoic acid could induce differentiation in affected cells (Breitman *et al.*, 1980), along with the discovery of retinoic acid receptor gene on chromosome 17 (Mattei *et al.*, 1988) led to the identification of the rearrangement itself by several groups (Alcalay *et al.*, 1991; Borrow et al., 1990; de The et al., 1990). The reciprocal gene on chromosome 15 at the q22 band was subsequently described as the promyelocytic leukemia gene product, or PML. It was later found that three other translocations involving the retinoic acid receptor were found to also cause APL. The three proteins are PLZF, NPM and NuMA (reviewed in (Slack & Gallagher, 1999)). However, because 99.9% of all cases of APL involve PML, the others will not be discussed in this thesis.

The translocation results in the production of two, in-frame, novel gene products; PML-RAR and RAR-PML (Borrow et al., 1990). PML-RAR is the larger protein of the two and the more important one in the development of APL. It includes the Ring finger, the two B-boxes and the coiled-coil domain responsible for multimerisation of the PML protein. It is also fused to most of the RAR protein,

including the DNA binding domain, the ligand-binding domain, the heterodimerization domain and the ligand-dependent activation domain. However, it lacks the ligand-independent activation domain of RAR. The consequence of the expression of this protein in cells is the disruption of the normal PML nuclear bodies into approximately one hundred smaller foci (< 0.1 um), termed microspeckles (Ferrucci *et al.*, 1997). These speckles are nuclear matrix bound and contain major components of PML nuclear bodies, such as Sp100 and PML as well as components of the retinoic acid receptor complex such as RXR (Weis *et al.*, 1994). The existence of these structures is likely to be a consequence of the fact that the PML-RARα has both the multimerization domain of PML and the heterodimerization domain of RARα. Because the fusion protein interferes with the expression of the normal allele of both PML and RARα, it functions in a dominant-negative manner. Subsequent studies have shown that it is not the disruption of the retinoic acid receptor pathway, but the disruption of the PML nuclear bodies that is responsible for the transformation by using a PML-RAR mutant with a non-functional activation domain (Kogan *et al.*, 2000).

The reciprocal product, RARα-PML, has a very limited portion of each protein. It consists of the ligand-independent activation domain of the RARα and a short region of PML containing a variety of serine-rich segments. The possibility of a functional role has been suggested, but it is very unlikely that this protein contributes in any way to the transformation process of cells (Slack & Gallagher, 1999).

The discovery of the translocation in the RARα gene suggested the use of all-trans retinoic acid (ATRA), a normal ligand for RARα, as a possible treatment for APL (Alcalay et al., 1991; Breitman et al., 1980; de The et al., 1991). The result was even better than what was originally expected. Treatment with ATRA of patients with APL resulted in a complete remission (Grignani *et al.*, 1994; Huang *et*

al., 1988). At the cellular level, the transformed myeloid precursors were able to undergo differentiation (Flynn *et al.*, 1983). At the subcellular level, the PML nuclear bodies are reformed and appear as normal structure (Koken et al., 1994). At the molecular level, the PML-RARα fusion protein was targeted for degradation (Raelson *et al.*, 1996; Yoshida *et al.*, 1996). This reorganization of the nuclear body structure, either as a consequence of or in association with PML-RARα degradation, appears to be a critical step in the differentiation process of APL cells. This concept is supported by data showing that ATRA-resistant APL cells fail to reorganize the PML nuclear body structure (Duprez *et al.*, 1996; Dyck et al., 1994). Moreover, overexpression in murine myeloid cells of a PML-RARα mutant that cannot activate transcription, but that can disrupt PML nuclear bodies, can still prevent differentiation (Kogan et al., 2000).

The discovery that PML expression can be induced after treatment with arsenic trioxide suggested a new possible treatment for patients with APL (Zhu *et al.*, 1997). It was of particular interest to use in the case of resistance to ATRA treatment. In APL cells, arsenic targets PML and PML-RARα into PML nuclear bodies and induces their degradation. Thus, ATRA and arsenic target RARα and PML, respectively, but both induce the degradation of the PML-RARα fusion protein, which should contribute to their therapeutic effects (Shao *et al.*, 1998; Zhu et al., 1997).

Transcriptional regulation by RARs involves chromatin modifications by histone deacetylases, which are recruited to RA-target genes by nuclear co-repressors (Nagy *et al.*, 1997). PML-RARα can recruit the nuclear co-repressor histone deacetylase complex through the RARα part of the protein. High doses of ATRA induce a release of this complex, thus activating transcription. Mutations of the binding site on RARα, as well as histone deacetylases inhibitors, abolish the ability of the PML-RARα protein to block differentiation. Therefore, recruitment of

histone deacetylase is crucial to the transforming potential of PML-RARα (Grignani *et al.*, 1998; Lai & Borden, 2000). Again, the understanding at the molecular level of the oncogenic protein, PML-RARα, allowed the finding of a new treatment for patients developing resistance to ATRA-only treatment (Kitamura *et al.*, 2000).

PML Nuclear Bodies and Viral Infection

PML nuclear bodies are a target of a variety of viruses, if not all, and are thought to be involved in coordinating the expression and replication of viral genomes from phylogenetically distinct families (Maul, 1998; Sterndorf et al., 1997a). The shape and the size of PML nuclear bodies is modified soon after viral infection. Moreover, they seem to be involved in the replication and the transcription of virusal DNA. The viruses known to have an effect on PML nuclear bodies are Herpes Simplex Virus, CytoMegaloVirus, Epstein-Barr Virus, Simian Virus-40, Influenza Virus A, Human T-Cell Leukemia Virus, PapillomaVirus and AdenoVirus (De Bruyn-Kops & Knipe, 1994; Desbois et al., 1996; Doucas *et al.*, 1996; Everett *et al.*, 1998; Everett & Maul, 1994; Ishov & Maul, 1996; Ishov *et al.*, 1997; Maul, 1998; Maul *et al.*, 1993; Sterndorf et al., 1997a).

Replication of viruses at the PML nuclear bodies

Because so many viral proteins interact in some way with the PML nuclear bodies, the replication cycle of several viruses has been analyzed. A number of DNA viruses, such as SV40, Ad5 and HSV-1 begin replication in the vicinity of a few, but not all, of the PML bodies in a nucleus. Increased amounts of infectious virus in a cell do not result in an increase in the number of nuclear sites of viral replication. This implies that PML nuclear bodies may not be identical (De Bruyn-Kops & Knipe, 1994; Maul, 1998). Viral protein expression does not appear to be necessary for targeting viral genomes to these replication sites (Ishov & Maul, 1996). This implies that there is a DNA sequence that is responsible for targeting

that DNA to the PML nuclear body. This is of particular interest since it represents a potential point of interference in viral replication (Ishov & Maul, 1996). The disruption of PML nuclear bodies, however, does not appear to be an essential step in the replication of the viral genome (Ishov & Maul, 1996; Maul, 1998). An interesting point is that PML nuclear bodies, as well as viral replication sites, have a symmetric position in daughter nuclei after division (Everett & Maul, 1994). This could be attributable to similar or mirror image positions of chromosomes observed in daughter cells after division (Rabl, 1885; Schardin *et al.*, 1985).

Transcription of viruses at the PML nuclear bodies

Early transcription of the viral genome also takes place exclusively at the periphery of the PML nuclear bodies, perhaps because they create a transcriptionally suitable environment (Ishov et al., 1997; Maul, 1998). The copy number of a viral genome that enters the nucleus appears to be larger than the number actually transcribed (Ishov & Maul, 1996; Ishov et al., 1997; Maul *et al.*, 1996), suggesting that a fraction are incapable of transcribing their genome, most likely because they are incapable of finding an environment suitable for transcription. The finding that transcription occurs at the PML nuclear bodies indicate that they are most likely competent sites for transcription.

Modification of PML nuclear bodies following viral infection

Many viruses disassemble or degrade PML nuclear bodies before proceeding to the late phase in infection cycles (Doucas et al., 1996; Ishov et al., 1997; Maul, 1998; Maul et al., 1996). Herpes simplex virus-1 (HSV-1) was shown to disperse PML nuclear bodies within two hours after infection (Maul et al., 1993). The immediate early gene 1 product (ICP0, IE110 or Vmw110) was shown to be necessary and sufficient for the disruption of PML nuclear bodies (Everett et al., 1998). This happens at the same time as the Vmw110 and proteasome dependent

loss of several PML isoforms (Everett et al., 1998; Everett *et al.*, 1999). Interestingly, this correlates with the proteasome-dependent degradation of the catalytic subunit of DNA-dependent protein kinase (Parkinson *et al.*, 1999). The protease that seems to be implicated in this process is HAUSP (Everett et al., 1999). It is also very probable that SUMO1 modification is implicated in the targeting process, although this remains to be shown. Dispersion of PML nuclear body components have been shown to be a common mechanism for many different viruses (Maul, 1998). The mechanism by which dispersion is achieved is unknown, but it was observed that viral proteins first localize to PML nuclear bodies for a relatively short period of time (1-4 hours). Following this targeting, the PML nuclear bodies are disrupted. This is done by most viruses studied so far and is typically achieved by only one of the viral proteins (Ishov & Maul, 1996; Ishov et al., 1997; Maul, 1998). It is very probable, since some of these viral proteins have been shown to interact with the protease involved in deSUMOlation, HAUSP, that SUMO1 is removed from the PML protein, thus preventing its targeting to PML nuclear bodies (Everett et al., 1998; Everett et al., 1999; Everett et al., 1997; Muller et al., 1998).

Biological Functions of PML

PML as a Growth and Tumor Suppressor

PML was shown to act as a tumor suppressor and as a growth suppressor both in vitro and in vivo. PML can inhibit transformation of rat embryo fibroblasts expressing Ha-ras and C-Myc (Mu *et al.*, 1994). The RING finger appears to be essential for the tumor suppressor capacity of PML (Le *et al.*, 1996). PML levels are cell cycle dependent, suggesting a possible function in regulating the growth rate. Indeed, overexpression of PML induces a sharp reduction in growth rates both in vitro and in vivo (Koken *et al.*, 1995). When malignant cells become invasive, they lose PML expression (Koken et al., 1995). The product of the BLM

gene is found to co-localize with the PML nuclear bodies. Bloom syndrome, a disease where the BLM gene is inactivated, shows an increase in genomic instability due to excessive chromosome breakage and chromatid exchange. In PML -/- cells, the BLM protein can no longer be localized to PML nuclear bodies and is found dispersed throughout the nucleus. These cells also show an increase in genomic instability, suggesting that PML nuclear bodies might also have a role in stabilizing genomic breaks (Zhong et al., 1999). The PML knockout mice show a higher rate of spontaneous papillomas and carcinomas, especially when treated with tumor inducers such as TPA (Zhong et al., 2000a). These findings show that PML might exert its tumor suppressing activity at multiple levels; by controlling cell growth, cell survival and genomic stability.

PML as a Pro-Apoptotic Factor

PML has been shown to participate in several different apoptotic pathways. Overexpression of PML in various cell lines results in increased apoptosis (Borden *et al.*, 1997; Fagioli et al., 1998; Quignon *et al.*, 1998), an activity that requires an intact RBCC domain (Borden et al., 1997). Interestingly, this mutant can no longer localize to PML nuclear bodies, but disrupts them, suggesting that the pro-apoptotic activity of PML requires intact nuclear bodies (Borden et al., 1997; Fagioli et al., 1998). Another protein found within PML nuclear bodies, Daxx also has pro-apoptotic activity. This protein was shown to interact directly with PML (Ishov et al., 1999; Zhong et al., 2000b). The PML -/- cells derived from the PML knockout mice are protected from multiple caspase-dependent apoptotic pathways such as Fas, tumour necrosis factor (TNF), ceramide, interferons and ionizing radiation (Wang *et al.*, 1998). However, the mechanism by which overexpressed PML leads to enhanced apoptosis appears to be caspase independent (Quignon et al., 1998). Moreover, the pro-apoptotic activity of Daxx is abrogated in the PML -/- cells (Zhong et al., 2000b). This shows that the PML nuclear bodies are essential in the caspase-dependent apoptotic pathways.

PML and the Immune System

PML is ubiquitously expressed in adult tissues at very low levels. However, treatment of cells with type I and II interferons, as well as many other stresses, induce the transcription of the PML gene dramatically (Chelbi-Alix *et al.*, 1995). It was shown that the promoter of the PML gene contains interferon-stimulated response elements (ISRE) (Stadler *et al.*, 1995). Sp100 is also induced upon exposure of cells to interferons (Sterndorf et al., 1997a). Upregulation of PML is also seen in inflammatory tissues (Terris, 1995). Moreover, PML is the target of many viruses. This all suggests that PML and the PML nuclear bodies are involved in the cellular defense pathways. Recent findings suggest that PML may be responsible for MHC class I expression in most cells, and MHC class II expression in lymphocytes (Schwiebert *et al.*, 1995; Zheng *et al.*, 1998). This implies that PML has a role in regulating antigen presentation, and would explain why viruses need to disrupt the PML body to prevent the infected cells from being recognized as expressing foreign proteins.

Fragments of foreign antigens associated with class I molecules of the major histocompatibility complex (MHC) are presented at the cell surface to elicit an immune response. This presentation requires the coordinated expression of several genes contained in the MHC locus, including those encoding the MHC class I heavy chain. The protein LMP-2 and LMP-7, which are involved in the proteasomal degradation of cytosolic antigens into peptide fragments that are destined for association with MHC class I molecules are part of the MHC locus. TAP-1 and TAP-2, which transport these fragments across the membrane of the endoplasmic reticulum at the start of their journey to the cell surface (York *et al.*, 1999) are also present in that locus. PML may be critical for MHC class I antigen presentation, either by regulating the expression of peptide transporter components (TAP1, -2, and LMP2, -7) to the MHC class I (Zheng et al., 1998), or by involvement in the construction of the antigen-MHC class I complex itself.

The MHC class II proteins play a central role in the development and maintenance of the immune system. They participate in the generation of the T cell repertoire in the thymus and are required for antigen presentation to T lymphocytes. MHC class II proteins are normally expressed on a limited number of cell types, which include B, thymic epithelial, dendritic, and glial cells, as well as activated macrophages (Flavell *et al.*, 1986). Corticosteroids are suppressors of the immune system, and one of the targets affected by corticosteroid is the expression of the MHC class II proteins (Schwiebert et al., 1995). It has been proposed that treatment with compounds such as the glucocorticoid receptor ligand dexamethasone causes the glucocorticoid receptor (GR) to tether the limited CBP to the GR elements. This causes a down-regulation of MHC class II expression, which also requires CBP as a co-activator (Fontes *et al.*, 1999; Kretsovali *et al.*, 1998; Schwiebert et al., 1995). Although there is no evidence connecting MHC class II expression and PML nuclear bodies, it is tempting to speculate that glucocorticoid receptor could recruit CBP out of PML nuclear bodies. It is, however, interesting to note that MHC class I expression and induction by interferons is still normal in PML -/- mice (Larghero *et al.*, 1999).

PML and Nucleoplasmic Transport of mRNA

PML has been proposed to be able to shuttle from the nucleus to the cytoplasm (Everett & Maul, 1994). Certain PML isoforms are cytoplasmic (Fagioli et al., 1992; Fagioli et al., 1998). A few reports described the ability of PML to accumulate in the cytoplasm under certain circumstances, such as viral infection (Campbell Dwyer *et al.*, 2000). Recently, it was demonstrated that PML was indirectly responsible for the regulation of export of some mRNAs, such as cyclin D1 mRNA (Campbell Dwyer et al., 2000; Lai & Borden, 2000). In this case, PML protein suppresses cyclin D1 protein production by altering the nuclear cytoplasmic distribution of cyclin D1 mRNA (Lai & Borden, 2000; Rosenwald *et al.*, 1995). This is achieved through direct interaction of PML with eIF-4E, a translation initiation

factor also responsible for exportation of some mRNA, such as cyclin D1 mRNA (Lai & Borden, 2000; Rosenwald et al., 1995; Rousseau *et al.*, 1996). Overexpression of PML causes an accumulation of eIF-4E within the nucleus, preventing the exportation of cyclin D1 mRNA (Lai & Borden, 2000). This could explain the growth suppressive activity of PML. Overexpression of PML, whether it is achieved by exogenous expression of a plasmid encoding PML or by interferon treatment, causes a decrease in cyclin D1 expression. This decrease in cyclin D1 expression is more likely to keep the cells in G1 phase, since cyclin D1 is responsible for the transition from G1 to S phase (Shackney & Shankey, 1999).

PML Nuclear Bodies Role in Transcription regulation

Even though PML has been shown to possess intrinsic transcription activation activity when tethered to DNA (Ahn *et al.*, 1998), it does not possess a DNA binding domain. It is then very unlikely that the PML protein itself is directly involved in transcription. However, other transcription factors or co-activators, such as Rb, p53 and CBP, can be found in PML nuclear bodies (LaMorte et al., 1998; Zhong et al., 2000a). The existence of nascent RNA polymerase II transcripts within this nuclear body has been reported (LaMorte et al., 1998). In addition, PML and the transactivation cofactor, CREB binding protein (CBP), colocalize within the PML nuclear bodies (Doucas *et al.*, 1999; LaMorte et al., 1998). Collectively, these findings support a role for this nuclear body in transcriptional regulation.

Hypothesis

The PML nuclear body is a well-studied nuclear structure, which may be a storage site for transcription factors, a site of transcription or a site of RNA accumulation. The presence of RNA, by fluorescein-UTP microinjection and EDTA-regressive staining, has been observed within the structure of the PML nuclear body (LaMorte et al., 1998), indicating a potential role in transcription or storage of RNA. These results implicate PML nuclear bodies either as sites of transcription or potential sources of transcription factors for surrounding transcriptionally active gene loci. Consequently, it is important to understand the composition of these structures and the composition and organization of the surrounding nucleoplasm. Until now, very poor characterization of the PML nuclear body and its surrounding has been achieved, using conventional approaches in transmission electron microscopy. What has been shown is that the PML nuclear bodies are spherical structures, approximately 250-500 nm in diameter (LaMorte et al., 1998; Stuurman et al., 1992). Using electron spectroscopic imaging and fluorescence microscopy, I intend to characterize the PML nuclear body and its surrounding, using phosphorus and nitrogen mapping. My hypothesis is that the PML body is a specialized region of the nuclear matrix, because of the insolubility of some of its components, and its function is to accumulate transcription regulatory factors.

It is not known how PML nuclear bodies are formed and it remains to be shown whether an underlying structural framework locally concentrates the components or whether the local accumulation results from random aggregations of rapidly diffusing components (Phair & Misteli, 2000). Specific proteins have been shown to associate and dissociate rapidly between the nucleoplasm and sub-nuclear compartments (Kruhlak *et al.*, 2000; Phair & Misteli, 2000); how such mobile proteins are concentrated within these compartments is not known. We have shown that nuclei that have not been exposed to extraction or other disruptive procedures possess a protein-based architecture (Hendzel *et al.*, 1999).

Surprisingly, such structures, which are completely devoid of nucleic acid, can be enriched in transcription regulatory factors (Hendzel et al., 1998). Whether these domains represent aggregations of randomly diffusing proteins, or are established by an underlying protein-based architecture, remains to be determined. I propose to study the mobility of different proteins of the PML nuclear body in order to determine if some of the proteins may play a structural role, whereas other proteins could be present only transiently. Since PML is the only protein that is sufficient and necessary for the formation of PML nuclear bodies, it is expected that it will have a structural role in the PML nuclear body. However, CBP would be expected to have a more functional role, being a transcription coactivator. The mobility of each of these proteins should reflect their specific roles.

Materials and Methods

Cell Culture Procedures

Cell Lines

A variety of cell lines have been used. The SK-N-SH (ATCC, HTB-11) are a human neuroblastoma of the brain and the metastatic site where they were collected is the bone marrow. HeLa cells (ATCC, CCL-2) are a human adenocarcinoma of the cervix. It has been shown that they are infected with the human papilloma virus-18 (HPV-18). 293 cells (ATCC, CRL-1573) are a human cell line from the kidney and have been transformed with adenovirus 5 sheared DNA. The 293T cell line is a variant of the 293 cells expressing the large T antigen. The Hs68 (ATCC, CRL-1635) primary culture is a human skin fibroblast culture from the foreskin of a newborn. The 10T1/2 cells (ATCC, CCL-226) are a primary culture from a mouse embryo.

Culture Media

Cells were grown in either Joklik's (JMEM) modification or Dubelcco's (DMEM) modification of Eagle's minimal essential medium (Gibco BRL). The medium was supplemented with 10% fetal bovine serum (FBS, Gibco BRL), as well as penicillin G (75 units/mL) and streptomycin (50 μg/mL). A 20 litre package was dissolved in 20 litres of milliQ filtered distilled water, along with 60 g of sodium bicarbonate. The medium was then sterilized by filtration. For transfection using Lipofectamine (Gibco BRL) or Lipofectin (Gibco BRL), the serum-free medium Opti-MEM (Gibco BRL) was used. However, for transfection with Lipofectamine 2000 (Gibco BRL), only antibiotic-free JMEM was used, supplemented with 10% FBS.

Plating

The cells were maintained as monolayers in 5% carbon dioxide at 37 °C, and divided before they reached confluence, using trypsin-EDTA (Gibco BRL, 0.05% trypsin (1:250), and 5mM EDTA). For immunofluorescence, coverslips were sterilized by bathing in ethanol, and allowed to dry under UV light for at least 15 minutes. The coverslips were then placed into 8-well dishes, and 2 mL of pre-warmed medium was added. Cells were then placed into the medium and allowed to adhere for at least 12 hours before use. For electron microscopy and correlative microscopy, cells were grown on polypropylene caps with 3 mL of medium.

Harvesting

Cells were harvested in SDS-PAGE as follows. Cells were washed twice with ice-cold PBS 1X, than scraped in 1 mL of PBS 1X with a rubber policeman. Cells were then pelleted by centrifugation for 1 minute at 2300g. The pellet was kept at –80 °C until usage.

Storage

For storage of cell lines, large flasks of cells were allowed to grow until they reached about 90% confluence. They were then trypsinized, pelleted by centrifugation in 15 mL conical tube (Falcon or Sarsted), and washed twice with PBS 1X. The pellet of cells was then resuspended in 93% fetal bovine serum (FBS, Gibco BRL) and 7% DMSO, transferred in cryogenic vials which were then sealed and incubated overnight at –70°C. The next day, the frozen vials were transferred to liquid nitrogen for long term storage. For thawing of cells, they were quickly thawed in hands and put directly into pre-warmed medium. The medium was then changed after 5 hours, or the following day.

Transfection of Mammalian Cells

For transient transfection, four different reagents were used; Lipofectin, Lipofectamine, Lipofectamine 2000 and Superfect. For Lipofectamine 2000, 2μg of DNA was diluted in 100uL of OptiMEM (Gibco BRL) and 5μL of Lipofectamine 2000 (Gibco BRL) was also diluted in 100μL of OptiMEM, in separate polypropylene tubes. After 5 minutes at room temperature, the two solutions were mixed and incubated for 20 minutes to allow complex formation. The mixture was then directly added to the 2mL of antibiotic free medium on the cells plated on glass coverslip. The medium was changed 5 hours after addition of the transfection mixture, and the cells were allowed to grow for 24 hours before fixation. The other reagents were used as recommended by the suppliers.

Antibodies

Antibodies against PML, Sp100 and CBP were used to detect PML nuclear bodies in cells. The PML mouse monoclonal antibody PG-M3 (Santa Cruz Biotechnology, Inc., sc-966) was used to recognize PML by Western blotting. However, this antibody did not recognize PML nuclear bodies by immunofluorescence. The mouse monoclonal 5E10 (Stuurman et al., 1992) recognized the same pattern of bands by western blotting as PG-M3, but also recognized PML nuclear bodies by immunofluorescence. The human antisera PBC-95 from a patient with primary biliary cirrhosis (gift from Dr. M. Fritzler, University of Calgary), recognized a protein of approximately 95 KD. We found, by overexpression of Sp100, that this antibody reacted against Sp100. Three rabbit polyclonal antibodies were used to recognize CBP. However, only antibodies recognizing the N-terminus of CBP provided the PML nuclear body pattern by immunofluorescence. The antibodies against the N-terminus of CBP are CBP-NT (A-22, sc-369, Santa Cruz Biotechnology, Inc.), CBP-NT (06-297, Upstate Biotechnology), and against the C-terminus, CBP-CT (06-294, Upstate

Biotechnology). The rabbit polyclonal antibody used to recognize p300 was against the N-terminus of the protein (N-15, sc-584, Santa Cruz Biotechnology, Inc.). The mouse and rabbit antibodies against Sam68, 7-1 and AD-1 respectively, were provided by Dr. S. Richard (McGill University) (Chen *et al.*, 1999). The rabbit polyclonal and mouse monoclonal antibodies against the glucocorticoid receptor (GR) are GR (E-20, sc-1003, Santa Cruz Biotechnology, Inc.) and Gr mAb250 (gift from Dr. JA Gustafsson, (Okret *et al.*, 1981)). The antibodies recognizing highly acetylated histones are the rabbit polyclonal anti-histone 4 on lysine 5 (06-759, Upstate Biotechnology) and anti-histone 3 on lysine 9 and 14 (06-599, Upstate Biotechnology). The antibodies recognizing Hemagluttinin A (HA) or FLAG tag are mouse anti-HA (12CA5, ATCC, 1013365), rabbit anti-HA (Y-11, sc-805, Santa Cruz Biotechnology, Inc.), mouse anti-FLAG M2 (F3165, Sigma-Aldrich). Interchromatin granule clusters (IGCs) were labelled using either a mouse monoclonal antibody recognizing the hyperphosphorylated form of the RNA polymerase II (CC-3, Dr. M. Vincent (Université Laval) (Vincent *et al.*, 1996)) or an antibody recognizing the splicing factor SC-35 (ATCC, 1023768).

The secondary antibodies were used for double labeling or triple labeling for immunofluorescence. For double labeling, a goat anti-rabbit Cy3 (Chemicon) and a goat anti-mouse (Alexa 488 Cedarlane or Cy2 Amersham) were generally used. For triple labeling, a goat anti-mouse Cy5 (Amersham), a goat anti-human Cy3 (Jackson Labs) and a goat anti-rabbit FITC (Chemicon) were used. For western blotting, a goat anti-rabbit or a goat anti-mouse coupled to horseradish peroxidase (HRP) was used (Jackson Labs).

Clones and cDNAs

The HA-tagged, mouse CBP cDNA was provided by Dr. Livingston (Harvard, Boston). It was cloned in the eukaryotic expression vector pRc/RSV plasmid (Invitrogen). The full reading sequence was subcloned, without the HA tag,

by cutting with BamH1. The cDNA was then inserted in the BamH1 site of pEGFP-C1, pEYFP-C1 and pECFP-C1, which tag a fluorescent protein to the encoded protein (Clontech). Dr. Evans provided the cDNA encoding the PML protein. It was already cloned in a vector with a GFP tag. The vector was developed by Dr. Evans' laboratory (Salk Institute) and is pCMX. Dr. Maul (Wistar Institute) provided the Sp100 cDNA cloned in the pCMX vector as well. It was cut out of this vector using HindIII – EcoRV. It was subcloned in pEGFP-C1, pEYFP-C1 and pECFP-C1 in the HindIII – SmaI sites. The vector expressing the HIV-1 Tat protein was provided by Dr. Verdin (UCSF). It was cloned in the pcDNA3.1 vector.

Electrophoresis

SDS-PAGE

Sodium dodecyl-sulfate polyacrylamide gel electrophoresis, or SDS-PAGE, was performed as described by Laemmli in 1970. The stacking gel was composed of 3.4% acrylamide (W/W); 0.09% bisacrylamide (W/W); 0.1% SDS, 145 mM Tris pH 6.8, 1 mg/mL ammonium persulfate (APS) and 0.05% (V/V) N,N,N',N'-tetramethylethyldiamine (TEMED). The resolving gel was composed of 6-12% acrylamide:bisacrylamide (29:1 ratio), depending on the size of the protein to resolved, 380 mM Tris pH 8.8, 0.1% SDS, 0.5 mg/mL APS, and 0.05% (V/V) TEMED. The gel size used was 9 cm width X 7 cm height X 1.5 mm thickness. The gel apparatus used was the MINI-PROTEAN II from Bio-Rad. The samples were prepared by adding boiled loading buffer (2X loading buffer: 100 mM Tris pH 6.8, 200 mM dithiothreitol (DTT), 4% SDS, 0.2% bromophenol blue and 20% glycerol) directly to the cell pellet. The samples were then boiled for 5 minutes and the DNA was sheared by vortexing for 30 seconds. Electrophoresis was carried on at 120 V for 1-2 hours, until the running dye had reached the bottom of the gel. Running buffer was composed of 25 mM Tris pH 8.5, 0.2 M glycine, 5% (V/V) glycerol and 0.1% SDS.

Transfer of Proteins to Nitrocellulose

Tranfer of proteins from a SDS-PAGE gel was usually to a nitrocellulose support membrane (Hybond-C Super, Amersham). The apparatus used was from the MINI-PROTEAN II (Bio-Rad) kit. The transfer buffer included 800 mL of distilled water, 3 g of Tris-Base, 14.4 g of glycine and 200 mL of methanol. The transfer was performed at 4 °C at 100 V for 1 hour, 50 V for 3 hours or 22 V overnight, depending on the situation.

Coomassie Staining

After completion of electrophoresis, gels were placed into a coomassie staining solution (1.0% (W/V) coomassie brilliant blue R-250 (Biorad), 10% (V/V) methanol, 15% (V/V) glacial acetic acid in distilled water), and rocked gently at room temperature for 1 hour. The gel was then washed with successive changes of destaining solution (10% (V/V) methanol, 15% (V/V) glacial acetic acid and 0.5% glycerol (V/V) in distilled water), usually overnight with pieces of paper to absorb the dye. Gels were then put between sheets of cellulose and allowed to dehydrated for a week.

Western Blotting

For probing the nitrocellulose membrane with antibodies (western blotting), the membrane was saturated with a blocking solution for at least one hour (TBST + 1% bovine serum albumin fraction V + 5% non-fat milk powder). TBST buffer contains 10 mM Tris pH 7.5, 0.5% (v/v) Tween 20 and 150 mM NaCl. The membrane was incubated with the primary antibody recognizing the desired protein for 1 hour at room temperature and washed 3 times with large volume of TBST, then incubated with the secondary antibody, coupled to HRP for 1 hour at room temperature. The antibodies were diluted in TBST. After the second incubation, the membrane was once again washed 3 times with TBST, then placed into a 1:1

ratio of the two solutions of the chemiluminescence reagent from NEN Life Science Products for 2 minutes. The membrane was placed into a saran wrap and allowed to develop on a KODAK BIOMAX MR film (VWR Canlab).

Agarose Gel

1% agarose gels were made by adding 1 g of dry agarose (Gibco BRL) to 100 mL of 1X TAE (Tris, acetic acid, EDTA) buffer, then boiled in a microwave until all the agarose was dissolved. The TAE buffer was made at 50X using 242 g of Tris base in 57 mL glacial acetic acid and 100 mL of 0.5 M EDTA pH 8.0 in a total of 1 L using distilled water. The solution was then poured into an agarose gel mould and allowed to cool at room temperature for approximately 30 minutes. The gels are run in 1X TAE buffer at 100 V until desired separation was achieved. Bands were visualized directly using an ultraviolet light source. The 6X loading buffer for the DNA samples contains 0.25% (W/V) bromophenol blue, 0.25% (w/v) xylene cyanol FF, 0.10% (w/v) ethidium bromide and 30% glycerol.

Cloning and Bacteriology Protocols

Propagation and Storage of Bacterial Cells and Plasmids

A variety of E.coli host strains were used in this work. The DH10B strain was used for electroporation. The XL1 blue, the DH5 alpha or the DH5 alpha with recA1 and endA1 mutations (Gibco BRL, 18265-107) were used for heat shock transformation. Master stocks of the host strains, or the host strains containing plasmid, were kept in 50% (V/V) glycerol at –80 °C in cryotubes. For propagation of bacterial cells, a small sample of the frozen stock was put into antibiotic containing media and incubated overnight at 37 °C with vigorous shaking. Antibiotic used was either ampicillin (100 μg/mL) or kanamycin (30 μg/mL). Plasmids were kept in water at –20 °C at high concentration (> 1μg/uL). The media used for propagation of bacteria were Luria Broth (LB) or Terrific Broth (TB). LB broth is composed of 10 g of tryptone, 5 g of yeast extract and 10 g of NaCl per

1 L of distilled water. Terrific broth is a richer variant of LB broth. It is made with 12 g of tryptone, 24 g of yeast extract and 4 mL of 100% glycerol per 1 L of distilled water. Salts were added after autoclaving and consist of 0.17 M KH_2PO_4 and 0.72 M K_2HPO_4.

Transformation of Bacterial Cells

For transformation of bacteria, two methods were used; heat shock and electroporation. For heat shock, 100 μL of competent XL1 blue or DH5 alpha were placed into a prechilled 15 mL Falcon tube and mixed with 10-50 ng of plasmid DNA. The cells were gently mixed and allowed to sit on ice for 30 minutes. The mixture was then incubated for 90 seconds at 42 °C and immediately put back on ice for 2 minutes. Following the heat shock, 1 mL of LB medium without antibiotic was added and the bacteria were allowed to recover at 37 °C for 1 hour with vigorous shaking. 100 μL of bacteria were then plated on LB agar plates containing the appropriate antibiotic. The plates were incubated overnight at 37 °C in an incubator.

For electroporation, DNA was precipitated and resuspend in distilled water to get rid of salts. 20 μL of electro-competent DH10B (Gibco BRL, 18290-015) were mixed with 5-20 ng of plasmid DNA. The mixture was then placed on ice for 5 minutes and then put into prechilled electroporation cuvettes. The bacteria were then electroporated using the BioRad Gene Pulser at the following settings: capacitance 500 μFD, resistance 200 OHMS and a potential difference of 1.70 Volts. Following the electroporation, 1 mL of LB medium without antibiotic was added and the bacteria were allowed to recover at 37 °C for 1 hour with vigorous shaking. 100 μL of bacterias were then plated on LB agar plates containing the appropriate antibiotic. The plates were incubated overnight at 37 °C in an incubator.

Small Scale Preparation of Plasmid DNA

Two methods were used for small scale preparation of plasmid DNA. The first one was the QIAprep Spin Miniprep Kit (QIAGEN, 27106). The starting volume of the bacteria culture used was 1.5 mL. The protocol supplied by the manufacturer was followed.

The second method used was a modification of the protocol suggested by Dr. Manfioletti (Del Sal *et al.*, 1989; Manfioletti & Schneider, 1988). Briefly, pelleted bacteria from a 2 mL overnight culture were resuspended in 200 μL of STET buffer (8% sucrose, 50 mM Tris pH 8.0, 50 mM EDTA, 0.1% (V/V) Triton X-100). 4 μL of a fresh solution of lysozyme (50 mg/mL of water) was added and lysis was allowed to proceed for 15 minutes. The samples were then boiled for 45 seconds and centrifuged for 10 minutes at 13000 rpm. The viscous pellet was remove manually with a tip or a toothpick. 5 μL of RNAse A (10 mg/mL) was added and the reaction was allowed to proceed for 10 minutes at 68 °C. Following this treatment, 20 μL of a CTAB (cetyl-trimethyl amonium bromide) solution (cationic detergent) was added and let to stand for 3 minutes (CTAB solution: 5% CTAB in a 0.5 M NaCl solution). The solution was then spun for 5 minutes at 13000 rpm. The pellet was resuspended in 100 uL of 1.2 M NaCl. 250 uL of ethanol was added and the solution was centrifuged for 5 minutes at 13000 rpm. The pellet was washed with 70% ethanol and the remaining plasmid DNA was resuspended in 50 uL of water.

Large Scale Preparation of Plasmid DNA

For large scale preparation of plasmid DNA (~1 mg), the QIAfilter Plasmid Maxi Kit (QIAGEN, 12262) was used. The starting volume of culture was usually

between 150 and 200 mL. The protocol supplied by the manufacturer was followed. The DNA was resuspended in 500 uL of milliQ filtered distilled water.

Agarose Gel Purification of DNA

Restriction endonuclease fragments of DNA separated on agarose gel were cut using a clean scalpel. The DNA fragment was then extracted from the piece of agarose gel using the QIAquick gel extraction kit (QIAGEN, 28704).

Precipitation of DNA with Ethanol

The DNA solution was precipitated by adding 1/6 volume of 0.3 M sodium acetate (pH 5.2) and 2.5 volume of ethanol. The mixture was allowed to incubate for at least 30 minutes at –20 °C. The DNA was then pelleted by centrifugation (minimum 13000g) for 30 minutes. The DNA was rinsed once with 70% ethanol to remove salts and re-spun for 10 minutes. The pellet was finally resuspended in the appropriate buffer.

T4 DNA Ligase Reactions

A molar ratio of 3:1 insert:vector was used for ligation of DNA. Purified insert DNA was mixed with the vector DNA in a minimum volume. 5X ligase reaction buffer was then added to a final concentration of 1X and 0.1 – 1 unit of T4 DNA ligase (Gibco BRL, 15224-025) was added. The reaction was allowed to proceed for 16-24 hours at 16 °C. The reaction was then diluted and used for transformation.

Preparation of Competent Cells

For heat shock competent cells, a single colony from a freshly grown plate was transferred into 100 mL of LB broth medium and incubated for 3 hours at 37 °C until the O.D.600 reach 0.5 - 0.8. The cells were then transferred into ice-cold 50 mL polypropylene Falcon tubes and incubated on ice for 10 minutes. The cells

were then spun down at 4000 g for 10 minutes. The pellets were resuspended in 10 mL of ice-cold 0.1 M $CaCl_2$ and stored on ice. The cells were once again spun down at 4000 g for 10 minutes. The pellets were resuspended in 1.5 mL of ice-cold $CaCl_2$ and aliquoted in 1.5 mL Eppendorf tubes and kept at –80 °C for long term storage.

For electro-competent cells, 1 liter of LB broth was inoculated with a 1/100 volume of a fresh overnight culture. The cells were grown at 37 °C until they reached an O.D.600 of 0.5 - 0.8, and then chilled on ice for 15 minutes. Cells were pelleted by centrifugation at 4000 rpm for 15 minutes. Pellets were resuspended in 1 liter of cold water and centrifuged as above, resuspended twice in 0.5 liter of cold water and centrifuged again. Pellets were resuspended in 20 mL of 10% glycerol, centrifuged again as above, and resuspended in 2 mL of 10% glycerol, aliquoted and kept at –80 °C for long term storage.

Microscopy Techniques

Immunofluorescence

Antibody labelling

Cells were cultured directly on glass coverslips under conditions recommended by the American Type Culture Collection. Cells were fixed with either 1.0% paraformaldehyde in PBS (pH 7.5) at room temperature for 5 min or –20 °C cold methanol for 5 minutes. Subsequently, cells were permeabilized in PBS containing 0.5% Triton X-100 for 5 min. Coverslips were then placed, cells facing down, on a 25 µL drop of a solution containing the diluted antibody (usually in PBS 1X) previously put on a parafilm sheet. Incubation was allowed to proceed for at least 30 minutes. The coverslip was then washed once with PBS 1X containing 0.1% Triton X-100, then twice with PBS 1X only. Cells were then incubated with secondary antibody and diluted as described for the primary antibody. After rinsing,

the samples were mounted in 1 mg/ml paraphenylenediammine in PBS/90 % glycerol containing the DNA specific stain, DAPI (Sigma), at 30 µg/ml.

Digital Deconvolution Confocal Imaging

Digital deconvolution confocal imaging was performed using a 14-bit cooled CCD camera (Princeton Instruments) mounted on a Leica DMRE immunofluorescence microscope. Images were recorded at steps of 0.1 to 0.5 µm. VayTek Microtome digital deconvolution software was used to remove out of focus contributions and image stacks were projected into one image plane using Scion Image software.

FRAP and FLIP Experiments

Fluorescence recovery after photobleaching (FRAP) and fluorescence loss in photobleaching (FLIP) experiments were done as follows. Coverslips were placed on glass slides containing several drops of medium surrounded by vacuum grease. The vacuum grease allows an airtight seal to form. Cells are capable of growing in these conditions for more than 24 hours at 22 °C. Individual cells were located by direct viewing through the microscope eyepieces. For FRAP, the laser scanning microscope (Zeiss LSM 510) was set to laser scanning mode and the initial imaging conditions were determined. A 25 X 0.8 numerical aperture (N.A.) lens was used for these experiments and pixel sampling was set between 90 and 120 nm per pixel. The argon laser spectral line at a wavelength of 488 nm was set to an intensity of no greater than 1.25 percent of its total power (15 mW) for image collection. A region, that typically covered half of the cell nucleus, was photobleached using 100 iterations at 100 percent laser intensity. 12-bit images were collected before, immediately following, and at defined intervals after bleaching. Since significant changes in GFP signal equilibrium were not observed

after 15 minutes, our total experiment time was set to 900 seconds to ensure that we observe complete recovery of photobleaching.

Labelling of Nascent RNA

Pulses of fluorouridine (FU) were performed by addition of fluorouridine to a final concentration of 2 mM in the culture medium. Antibodies against halogenated UTP (anti-BrdU, Sigma # B-2531) was used to label fluorouridine.

Image Processing

For false coloring, level adjustment and creation of panels, images were imported in Adobe Photoshop v5.0 or v5.5, converted from 12 bit images (in a 16 bit format) to 8 bit images. False colors were added by changing the image mode to indexed color, and the color mode to the desired RGB (red-green-blue) mixture. Typically, DAPI was shown as cyan (red = 100, green = 200, blue = 255), GFP, Cy2, FITC and Alexa488 as green (red = 0, green = 255, blue = 0), Cy3 as red (red = 255, green = 0, blue = 0) and Cy5 as purple (red = 255, green = 0, blue = 255). For superimposition, the recipient image was converted to a RGB mode, and the second image was pasted over. The blending mode used to see two color channels is "screen". The resulting colored images were then copied into a larger RGB file and saved in a TIFF format. For quantification of immunofluorescence signal, masks were drawn around individual nucleus or region of interest, and the signal intensity was integrated to get an average value using ErgoVista v4.4 image analysis software (Atlantis).

Correlative Microscopy and Electron Microscopy

Embedding and Labelling

Detailed descriptions of the electron microscopy procedure are presented elsewhere (Bazett-Jones & Hendzel, 1999). Briefly, cells were grown on polypropylene caps, fixed with 1.0% paraformaldehyde in PBS and labelled for immunofluorescence as described above. Cells were then re-fixed in 2% glutaraldehyde in PBS for 5 min, dehydrated in ethanol, starting at 30%. Ethanol was then replaced by Quetol 651 (Cedarlane, 20440) for at least 2 hours, followed by inflitration with Quetol 651-NSA-NMA-DMP30 mixture for 12 hours (Nonenyl succinic anhydride, NSA, Cedarlane, 19050 and Nadic methyl anhydride, NMA, Cedarlane, 19000). The mixture was prepared by mixing 35 mL of Quetol 651, 54 mL NSA and 11 mL NMA. DMP-30 is the catalyzer for the reaction and is used at 2% (V/V) in the mixture (2,4,6-Tri(dimethylaminomethyl)phenol, Cedarlane, 13600). Polymerization requires a further incubation of 48 hours at 60 oC.

Ultramicrotomy

Sections of approximately 30 nm and 90 nm thickness were obtained by ultramicrotomy with a diamond knife (Drukker). The sections were placed directly onto finder grids. Electron micrographs were obtained with a Gatan 14-bit slow scan cooled CCD detector on a Zeiss EM 902 transmission electron microscope equipped with an imaging spectrometer (Bazett-Jones & Hendzel, 1999).

Quantification and Image Analysis

To quantify phosphorus and nitrogen signals, regions containing resin only were used to estimate exposure times, such that images recorded at different regions of the energy loss spectrum, had equal background intensities. Masks were drawn around individual structures or regions and the integrated signal intensities spanning the phosphorus and nitrogen ionization edges were determined at 10 eV steps using ErgoVista v4.4 image analysis software.

Results

Chapter 1 : Characterization of the structure of the PML nuclear body.

Overview

PML nuclear bodies may be sites of storage of transcription factors, sites of transcription or sites of RNA accumulation. The presence of RNA, by fluorescein-UTP microinjection and EDTA-regressive staining, has been observed within the structure of the PML nuclear body (LaMorte et al., 1998), indicating a potential role in transcription or storage of RNA. These results implicate PML nuclear bodies either as sites of transcription or potential sources of transcription factors for surrounding transcriptionally active gene loci. Consequently, it is important to understand the composition of these structures and the composition and organization of the surrounding nucleoplasm. Until now, very poor characterization of the PML nuclear body and its surrounding has been achieved, using conventional approaches in transmission electron microscopy. What has been shown is that the PML nuclear bodies are spherical structures, approximately 250-500 nm in diameter (LaMorte et al., 1998; Stuurman et al., 1992). Using electron spectroscopic imaging and fluorescence microscopy, we have shown that the core of the PML nuclear body is a dense protein structure that does not contain any detectable nucleic acid. However, nascent RNA can be detected at the periphery, indicating that the surroundings of the PML nuclear bodies are sites of transcriptional activity.

Structure of the PML Nuclear Body by Correlative Microscopy

It has been reported that PML nuclear bodies are sites of transcription and RNA accumulation (LaMorte et al., 1998). We chose to test this model and to extend the model to higher resolution by direct visualization without using heavy atom contrast agents. We used electron spectroscopic imaging (ESI) to map

protein-based and nucleic acid-based regions in and around PML nuclear bodies. One advantage of this technique is that comparisons of nitrogen and phosphorus maps provide the ability to directly distinguish protein from nucleic acids *in situ*. Second, it is possible to quantify mass contributions from both the protein and the nucleic acid components of a structure and to map the spatial relationships of protein- and nucleic acid-based structures within the complex nuclear environment (Bazett-Jones & Hendzel, 1999). Third, the heavy atom contrast agents, which limit resolution and stain different biochemical components in a non-uniform or unpredictable manner, can be avoided.

Positive identification of PML nuclear bodies amongst other nuclear structures is difficult with ESI alone. To identify these structures definitively, we first labelled cells with antibodies against the N-terminus of CBP, which we have shown to co-localize with PML in PML nuclear bodies in SK-N-SH cells by immunofluorescence microscopy. Indeed, in this cell line, CBP is as reliable a marker of PML nuclear bodies as the PML protein itself. After embedding and thin sectioning, the same section can first be examined in the fluorescence microscope to identify the location of PML nuclear bodies in individual cells. The same section is then imaged at high resolution in the energy-filtering electron microscope (Bazett-Jones & Hendzel, 1999). A thin section showing a nucleus imaged by immunofluorescence is shown in Figure1A. Five PML nuclear bodies can easily be identified. Two are indicated (long and short arrows, Figure1D and E) near the nucleolus (Nu, Figure 1A, D and E). The same section imaged at 155 eV energy loss is shown in Figure1B at low magnification and superimposed with the immunofluorescence image in Figure1C, to correlate the fluorescently labelled structures with the underlying ultrastructure. Two PML nuclear bodies are then detectable in the high magnification phosphorus (Figure 1D) and nitrogen (Figure 1E) maps. The core of this nuclear body is well contrasted in the net nitrogen image, whereas the phosphorus content is low, indicating that the core is mainly composed of protein.

The core of the PML nuclear body is a protein-based structure

Qualitative analysis of such images (Figure 1D,E) indicates that the core of the PML nuclear body is depleted in nucleic acids. Figure 2 shows high magnification images of a PML nuclear body (left, Net P; right, Net N). The presence of RNA or DNA in this structure would likely resemble phosphorus-rich granules, as seen in the core of the interchromatin granule clusters and throughout the nucleoplasm (Bazett-Jones et al., 1999; Hendzel et al., 1998), or more extended fibrils reflecting noncompacted nucleic acids (Hendzel et al., 1999). Such structures are not apparent even at high magnification (Figure 2). To extend the morphological analysis, we quantified the phosphorus and nitrogen content in different regions around the PML nuclear body (Figure 2B and D). The core of the PML nuclear body, a region corresponding to condensed chromatin, a background region in the nucleoplasm, and a background outside of the cell comprised of the embedding resin alone (not shown) were delineated with masks. The signal spanning the phosphorus $L_{2,3}$ and nitrogen K edges were integrated over the regions delineated by the masks (Figure 2B and D). The energy loss spectra of regions in the nucleus are consistent with the presence of phosphorus, characterized by the strong delayed edge above 150 eV. The phosphorus content (155 eV) of the core of the PML nuclear body was approximately 1.4% above the nucleoplasmic background, whereas the chromatin was 16% above the nucleoplasmic background, corresponding to a signal 11 times higher for the chromatin compared to the PML nuclear body. In contrast, the nitrogen signal (415 eV) for chromatin is 9% over the nucleoplasm and the PML body core is 10% over the nucleoplasmic background. The phosphorus signal in the nucleoplasmic background is likely derived predominantly from phosphorylated proteins. Because of a comparable phosphorus signal in the PML nuclear body core and the nucleoplasm, and the absence of morphologically recognizable phosphorus-rich complexes, we conclude that the core of this subnuclear structure is composed only of protein.

Structure of the Sam68-SLM nuclear bodies by correlative microscopy

Sam68, or SRC associated in mitosis protein of 68 KDa, is a substrate for Src kinases during mitosis (Fumagalli *et al.*, 1994). Sam68 is an RNA binding protein that is found in the nucleus (Ishidate *et al.*, 1997), but localizes in novel nuclear structures in cancer cell lines (Chen et al., 1999). Because this protein can bind RNA, we expected that this nuclear structure would contain nucleic acid, and thus serve as a positive control for nucleic acid detection. Indeed, we found that Sam68 nuclear bodies are enriched in both phosphorus and nitrogen-rich fibers, indicating the presence of nucleic acids (Net P and Net N images, Figure 3). These structures, as seen by immunofluorescence and electron microscopy, are large, spherical or ovoidal structures of approximately 0.5 to 1 μm in diameter. Because the Sam68 nuclear bodies contain nucleic acid, this structure serves as a positive control to show that phosphorus signal can indeed be detected by electron spectroscopic imaging.

Phosphorus-rich fibers are present at the periphery of the core of the PML nuclear body

Although the use of thin sections (30 nm) is necessary for quantitative elemental analysis by ESI, we have found that thicker sections stained with uranyl acetate still contain qualitatively useful elemental information (Boisvert *et al.*, in preparation). Thicker sections allow one to follow fibers that would otherwise rapidly leave the plane of the section if they are not parallel to the section. Figure 4 shows consecutive 90 nm sections through a PML nuclear body. The centre of the PML body core is characterized by a hole in the nitrogen map (arrow, Figure 4.1). Blocks of condensed chromatin surrounding the core are evident in the phosphorus-enhanced maps (arrows, Figure 4.1, 4.2; Figure 2A). Extended thin fibers measuring as little as 2 nm in diameter can often be visualized at the immediate periphery of the core of the PML nuclear body when imaged with high

resolution (Figure 5). Nascent RNA is the most abundant sub-nuclear structure that has been identified in an extended conformation (Malatesta *et al.*, 1994), and it is likely, therefore, that these phosphorus-rich fibres are RNA-based.

Localization of Nascent RNA at the Periphery of the PML Nuclear Bodies

Our ESI analysis indicates that the core of the PML nuclear body is composed mainly of protein, whereas the periphery contains DNA and/or RNA. Previously, the entire PML body was reported to contain RNA (LaMorte et al., 1998). To determine whether newly transcribed RNA is present in the vicinity of PML bodies, we labeled cells with fluorinated uridine (FU). Incorporation of FU in nascent RNA is rapid and specific. Signal visualized with antibodies against halogenated nucleotides, can be detected throughout the nucleoplasm after 2 minute pulses, with increasing signal over time (Figure 6C, H, M). Strong, but less punctate nucleolar labelling can also be seen after 10 minutes, concordant with the high level of transcription therein. This observation indicates that the penetration of the antibody and the FU is not inhibited by dense, compartmentalized structures such as the nucleolus. To determine the relationship between PML nuclear bodies and RNA synthesis and accumulation, we co-labelled cells with anti-CBP N-terminal antibodies (red, Figure 6B, G, L) and anti-FU antibodies (green, Figure 6C, H, M) after 2, 10 and 60 minute pulses of FU. After only 2 minutes, most PML nuclear bodies have FU incorporated RNA on their peripheries. When pulses were extended to longer times, RNA is still seen on the periphery in a small number of foci, and does not accumulate inside the structure as visualized by CBP labelling (Figure 6E, J, O). We conclude that the core of the PML nuclear body is a protein dense structure surrounded by sites of RNA transcription.

The Chromatin Surrounding the PML Nuclear Bodies is highly acetylated

To determine whether the region surrounding the PML nuclear body is transcriptionally or potentially active, or whether the PML nuclear body contains

actively transcribed chromatin that was not detected in other experiments, we co-labelled cells with an antibody against the PML protein (Figure 6Q), and with an antibody recognizing the transcription-associated, highest acetylated species of histone H3 (Figure 6R) (Boggs *et al.*, 1996). As expected from the fluorouridine incorporation experiments and ESI analysis, the core of the PML nuclear body did not show any evidence of highly acetylated euchromatin. All of the PML nuclear bodies, however, were within one diameter (250 nm) of a block of highly acetylated chromatin (Figure 6S). This would not be observed with a random distribution of PML nuclear bodies. Moreover, some PML nuclear bodies were associated with multiple blocks of acetylated chromatin (Figure 6T) (also see blocks of chromatin surrounding the PML nuclear body in the net phosphorus image (Figure 2A)). This indicates that the active chromatin is often physically separated from the core of the PML nuclear body by a narrow intervening shell that is depleted in chromatin. This result is consistent with the ESI images, in which the chromatin domains are separated by an intervening space that contains RNA. The variability in the amount of acetylated chromatin associated with each PML body may indicate different levels of transcriptional activity between these domains. Most of the PML nuclear bodies, however, are surrounded by acetylated chromatin (Figure 6S), indicating that the periphery of the PML nuclear bodies is a site of transcription. The absence of highly acetylated chromatin or DAPI-stained chromatin within the core of the PML nuclear body indicates that the core of the structure is not a site of transcription.

Figure 1 Identification of PML nuclear Bodies by Correlative Microscopy.

Cells were labeled with anti-CBP-NT antibody, embedded and sectioned. Sections are first imaged by immunofluorescence microscopy (A). It is then possible to image the same section by electron microscopy using ESI (B). The images are resized and rotate for proper alignment before being merged (C). Immunofluorescence microscopy also serves to identify and locate structures of interest, so that these can be analyzed at the ultrastructural level by ESI, to map phosphorus (D), and nitrogen (E). The region indicated by the box in (C) is magnified in (D) and (E). Arrows in (D) and (E) represents the two PML nuclear bodies in (C). A nucleolus is shown in (D) and (E) as Nu and represent a structure rich in both phosphorus and nitrogen.

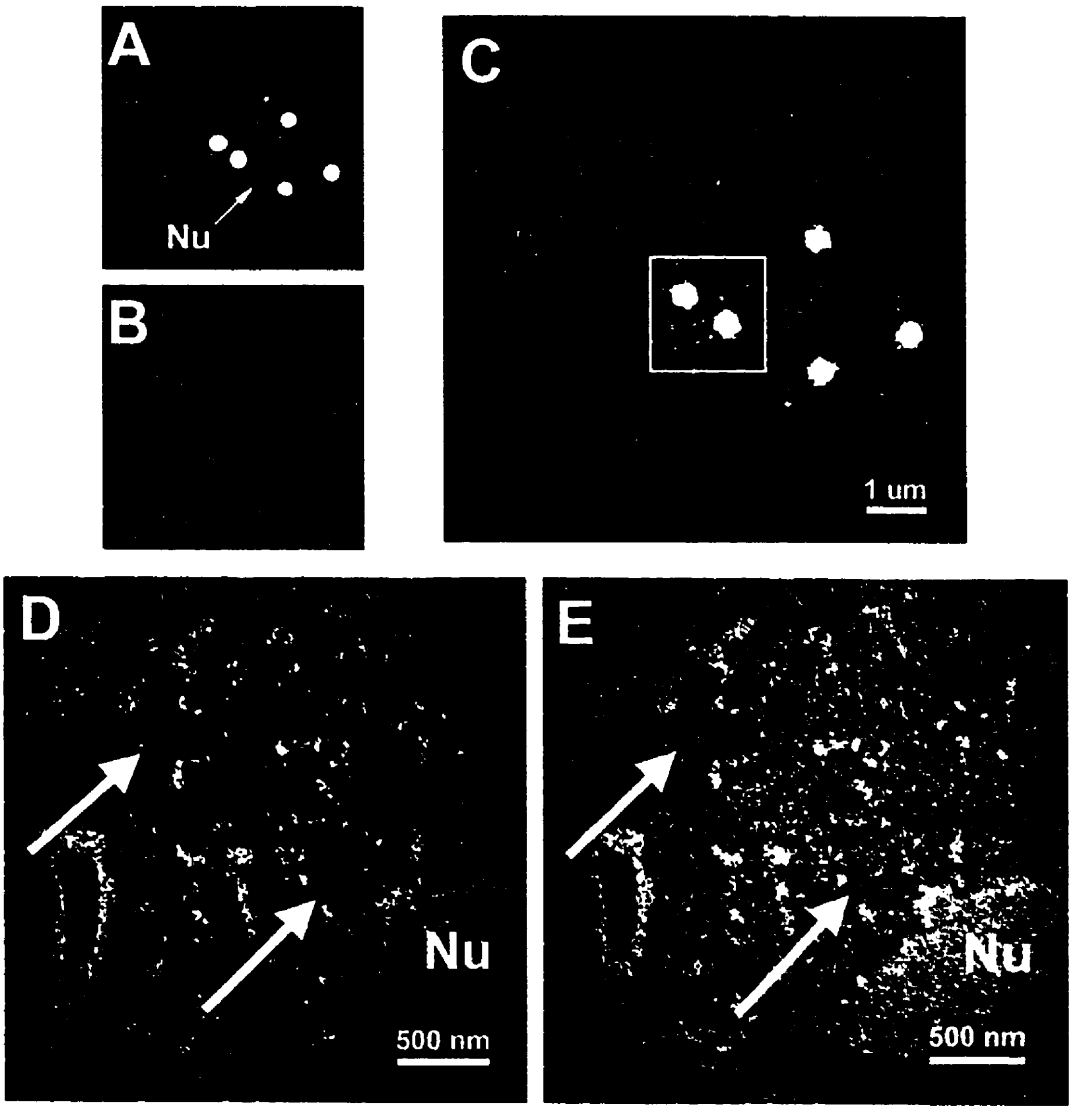
A
Nu
B
C
1 um
D
Nu
500 nm
E
Nu
500 nm

Figure 2 Quantification of Phosphorus and Nitrogen Content of a PML Nuclear Body.

The three indicated areas were used for quantification of phosphorus and nitrogen. The left region corresponds to chromatin, the middle region to nucleoplasm, and the right region to the core of a PML nuclear body. A fourth region (not shown) corresponds to a region outside the cell, containing only the embedding resin. The net phosphorus image is shown in (A) and the net nitrogen image in (C). Energy loss spectra of these regions spanning the phosphorus $L_{2,3}$ edge (B) and the nitrogen K edge (D) are presented at 10 eV intervals.

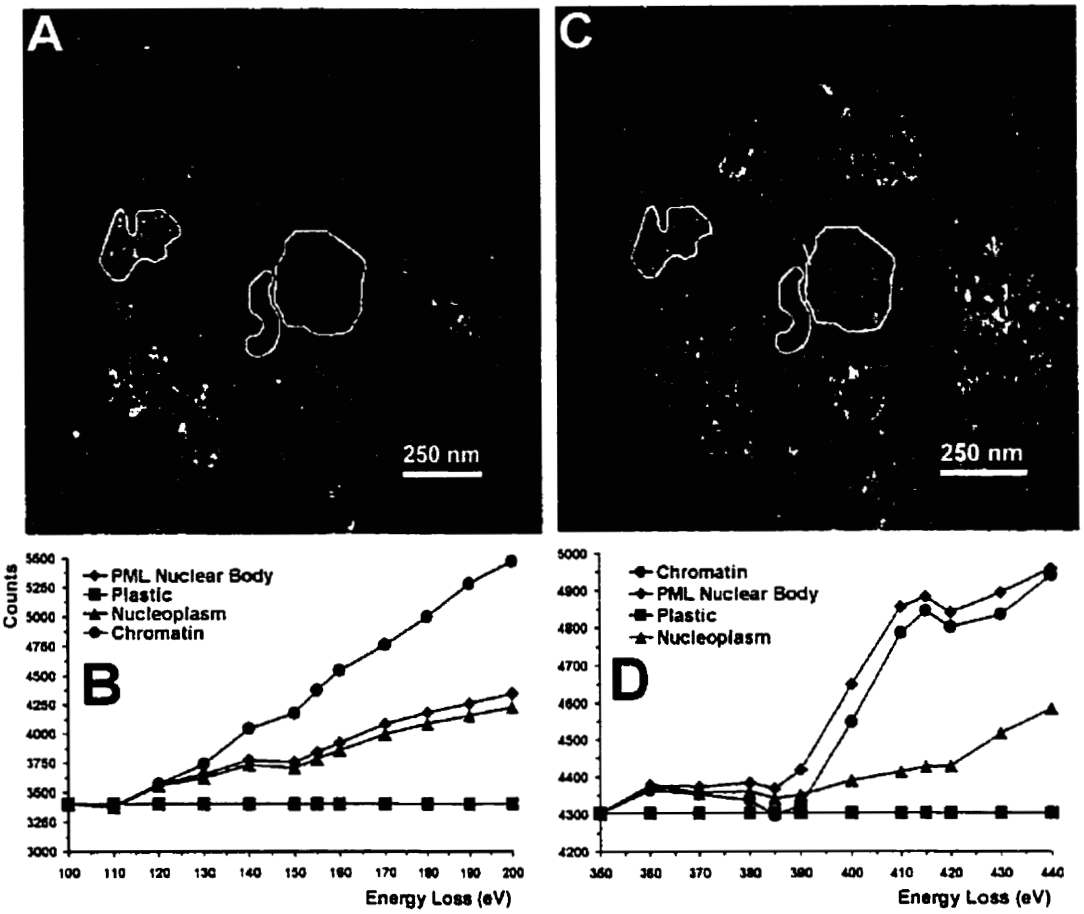
A
250 nm
C
250 nm
B
PML Nuclear Body
Plastic
Nucleoplasm
Chromatin
Counts
Energy Loss (eV)
D
Chromatin
PML Nuclear Body
Plastic
Nucleoplasm
Energy Loss (eV)

Figure 3 Characterization of Sam68 Nuclear Bodies by Correlative Microscopy
An ultrathin section (30 nm) of HeLa cells, previously labeled with anti-Sam68 AD1 antibody and embedded for electron microscopy, was examined under an immunofluorescence microscope (A) and then under an electron microscope (B). The respective images are resized and rotationally aligned before being merged (C). It is then possible to identify the location of structures labeled by immunofluorescence and to characterize them, by ESI, for phosphorus content (D) and for nitrogen content (E). (Magnification: B and C are 3000X; D and E are 12000X).

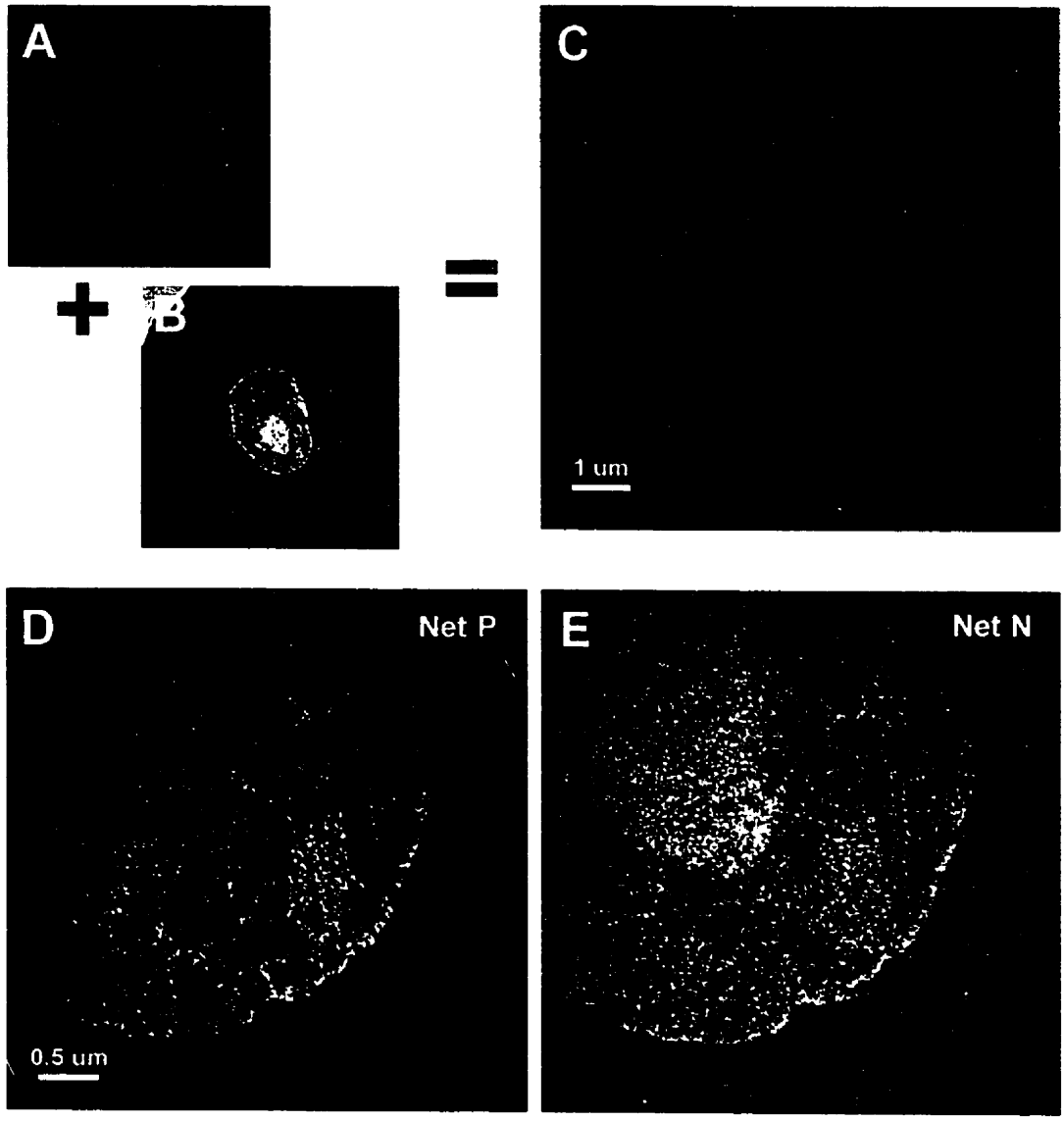
A
B
C
1 um
D
Net P
0.5 um
E
Net N

Figure 4 Serial sections of 90 nm thickness of a PML nuclear body stained with uranyl acetate.

Images in the left column are phosphorus enhanced, recorded at 155 eV, and those in the right column are nitrogen enhanced, recorded at 415 eV. The middle of the PML nuclear body is shown in section (1). The protein core is visible in the nitrogen enhanced image, and a hole on the core is indicated with the arrow in the nitrogen enhanced image. Arrows in the phosphorus enhanced images indicate blocks of condensed chromatin. The next section, (2), still shows the protein core, whereas section (3) is now out of the core of the nuclear body. The last section, (4), shows the chromatin closing back over the structure.

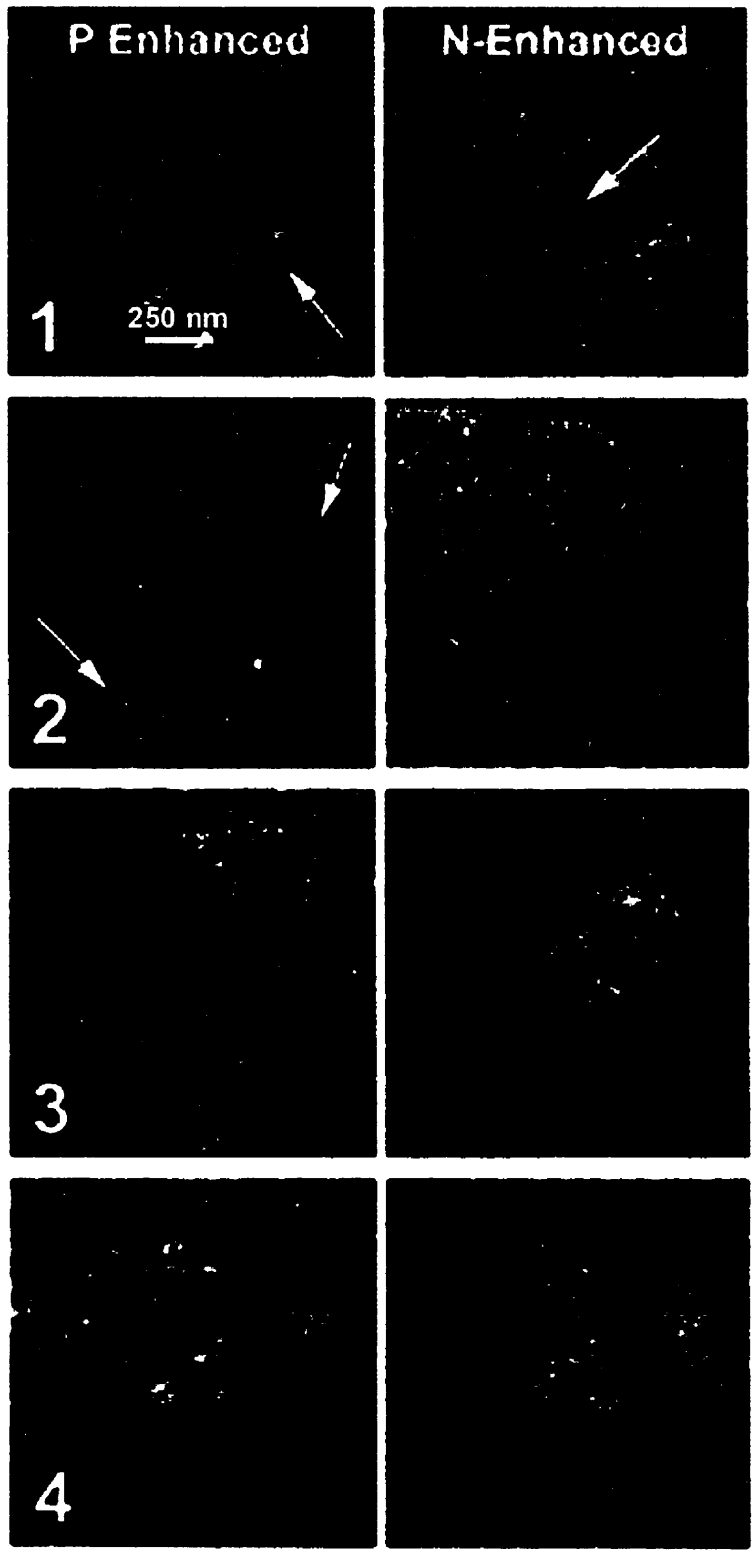
P Enhanced
N-Enhanced
1
250 nm
2
3
4

Figure 5 Thick section of a PML nuclear body, stained with uranyl acetate

A thick, uranyl acetate stained section was recorded at 415 eV at high magnification (85,000X). The enhanced nitrogen image is shown. Extended fibers are observed just outside the core of the PML nuclear body. These fibres are approximately 2-4 nm in diameter, and are also phosphorus-rich (not shown).

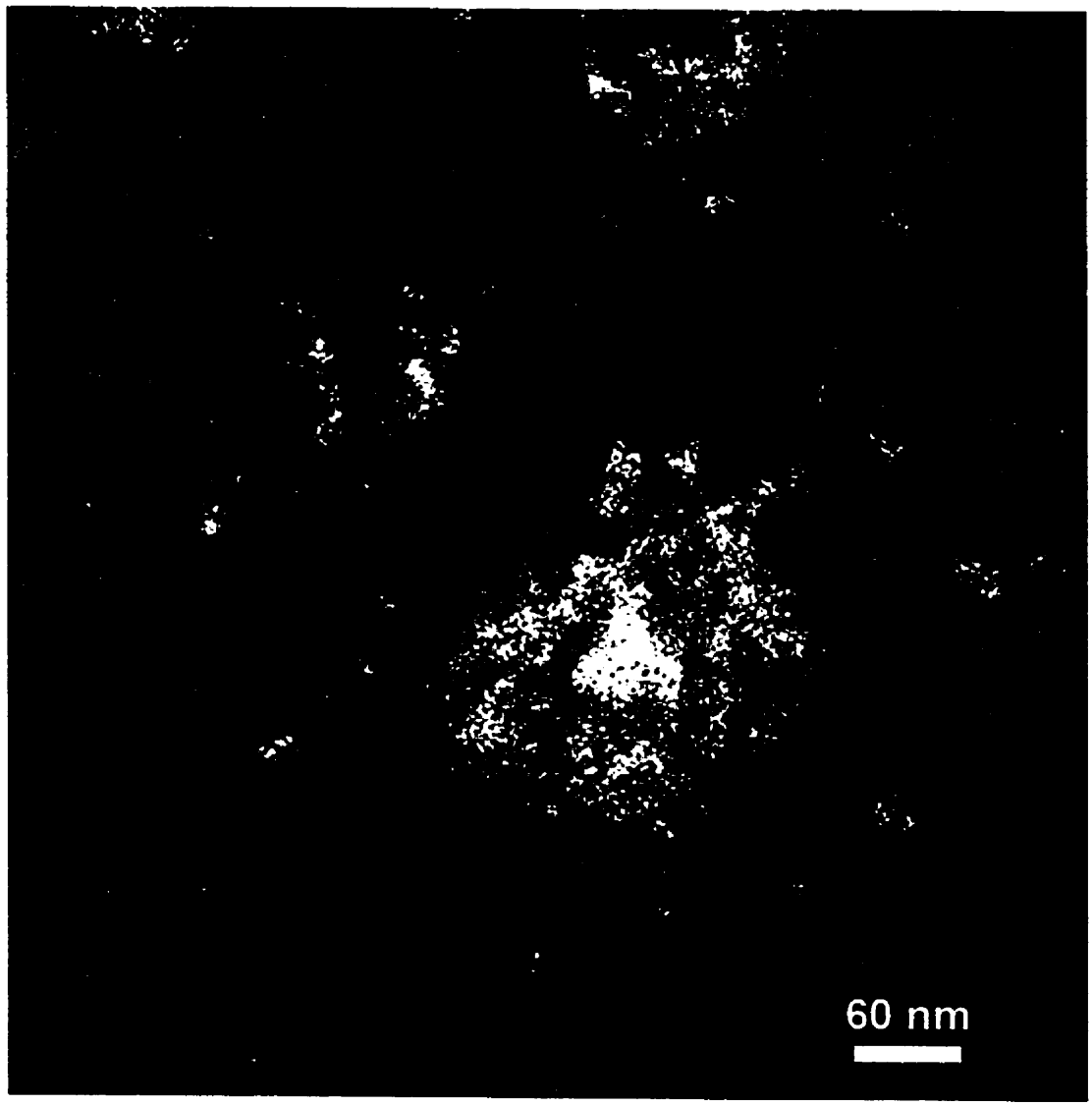
60 nm

Figure 6 Confocal Microscopy of Cells Showing Nascent RNA and Acetylated Chromatin

Confocal microscopy of SK-N-SH cells pulsed with fluorouridine for 2 (A to E), 10 (F to J) or 60 (K to O) minutes. Fluorouridine was labeled with an anti-BrdU antibody (green, C, H, M) and anti-CBP-NT antibody (red, B, G, L). Merged images are shown (D, I, N) and a high magnification of one PML nuclear body for each time course are displayed (E, J, O). DNA stained with DAPI shows the nucleus of each cell (A, F, K, and P). Some cells were labeled with an antibody against the highest acetylated form of histone H3 (green, R) to reveal transcriptionally active/competent chromatin. PML nuclear bodies were detected with an antibody against PML protein (5E10) shown in (Q). Images (P), (Q) and (R) are merged to form (S), and the indicated PML nuclear body is magnified in (T). Arrows in (D), (I), (N) and (S) points the PML nuclear bodies that have been zoomed in (E), (J), (O) and (T).

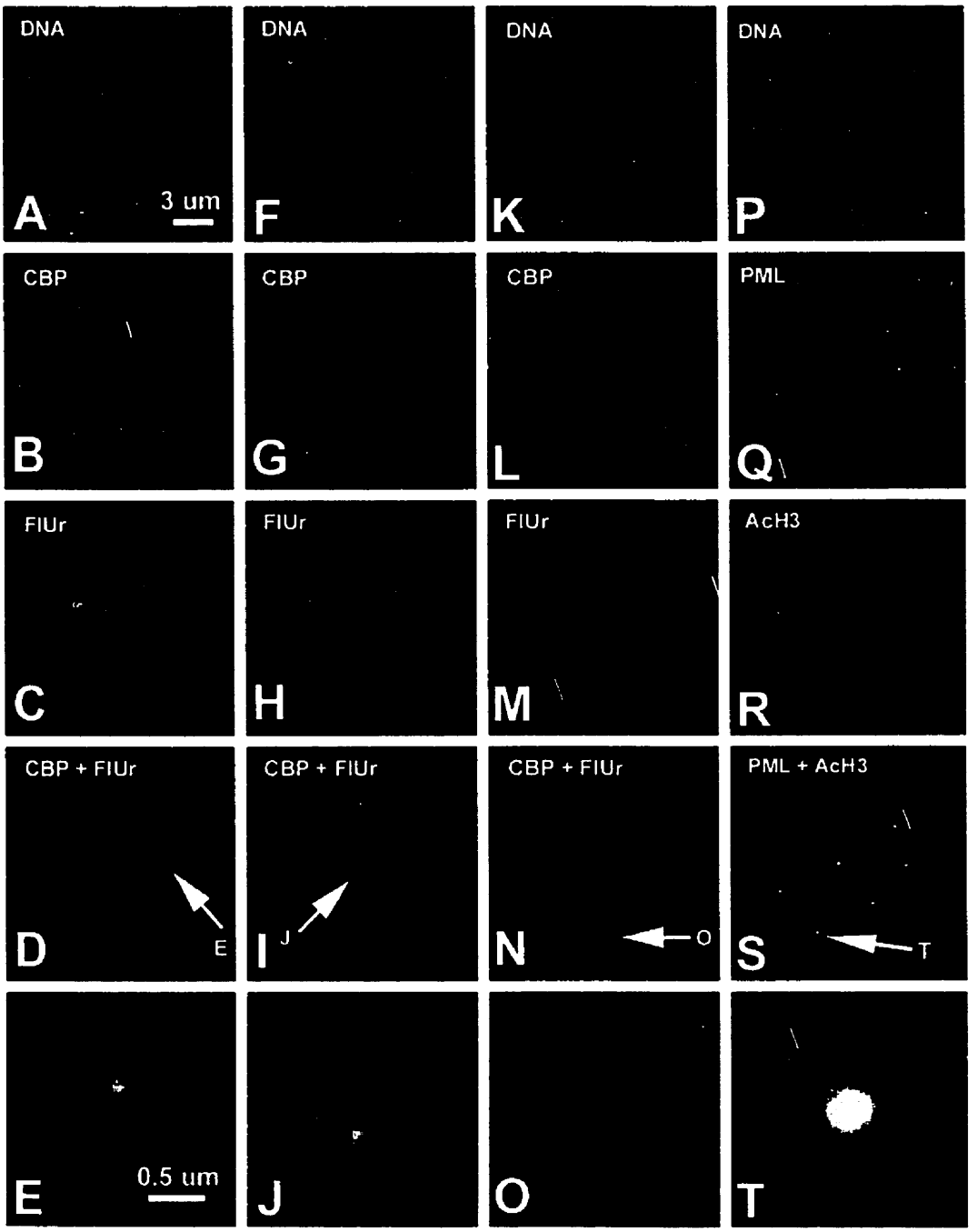
DNA
A
3 um
DNA
F
DNA
K
DNA
P
CBP
B
CBP
G
CBP
L
PML
Q
FIUr
C
FIUr
H
FIUr
M
AcH3
R
CBP + FIUr
D
E
CBP + FIUr
I
J
CBP + FIUr
N
O
PML + AcH3
S
T
E
0.5 um
J
O
T

Discussion

There has been an increasing interest in PML nuclear bodies in the past few years because of their involvement in viral infection (Maul, 1998; Sterndorf et al., 1997a; Zhong et al., 2000a), and their disruption and disappearance in acute promyelocytic leukemia (de The et al., 1991; Kakizuka et al., 1991). Whether this structure serves only as a storage site for regulatory factors, functions as a site for transcription by creating a suitable environment, or plays some other role, will only be determined as its structure and composition are characterized. In this chapter, I have addressed several questions about the structure and the organization of the PML nuclear body.

First, I have shown that the core of the PML nuclear body is composed entirely or almost entirely of protein. There is no detectable nucleic acid in the 250 nm diameter core of the structure. This protein core is not a uniform sphere of protein, but rather has channels and pores throughout. Serial sections (Figure 4) indicate that the mass density of the very centre is much lower than the outer regions of the protein-based core. Many proteins have been shown to localize to PML nuclear bodies, such as the transcription regulatory factor PML protein, the transcriptional co-activator CBP, and other proteins such as Sp100. It is likely that such components of the PML nuclear body are localized in this core structure, and the core represents a specialized component of the nuclear protein architecture/matrix (Hendzel et al., 1999). The protein-based core is surrounded by blocks of chromatin that is condensed to levels beyond the 30 nm fibre. In cross-sections, phosphorus maps illustrate a ring of chromatin that forms a halo around the protein-based core, and phosphorus maps of serial sections demonstrate that the chromatin forms a shell, which completely surrounds the core. Some of this chromatin is enriched in the highly acetylated forms of histone H3, a good marker for transcriptional activity (Boggs *et al.*, 1996; Hendzel et al., 1998). If transcriptionally active chromatin is found on the periphery of the PML

nuclear body, then it should be possible to detect nascent RNA at this location. Indeed, nascent RNA can be detected on the periphery but not inside the protein core of the nuclear body. Even after long incubations in the presence of label, the core of the structure remains free of RNA. We also observe fibres in the space between the protein core and the surrounding chromatin, fibres that are phosphorus-rich and are morphologically more consistent with being RNA than chromatin. The presence of nascent RNA at the periphery of this structure is concordant with the observation by Maul and coworkers (Ishov et al., 1997) who localized viral transcripts next to this nuclear body.

My conclusions differ dramatically from those of LaMorte and co-workers (LaMorte et al., 1998). These authors used EDTA-regressive staining technique, which preferentially labels RNA (Bernhard, 1969), and fluorescein-UTP incorporation in *in situ* nuclear run-on experiments to conclude that very high concentrations of RNA are localized within the structure. Both experiments have limitations. The specificity of the EDTA-regressive staining procedure is not absolute, and in the case of structures of unknown composition, cannot be interpreted to be RNA-based solely on the presence of staining after the EDTA chelation of uranium ions from chromatin (Bernhard, 1969). We report here that the core of the PML nuclear body contains only nucleoplasmic background levels of phosphorus and no discernable phosphorus-rich fibers. This holds for all PML nuclear bodies observed and does not characterize a small subset of these structures (LaMorte et al., 1998). As a positive control for our observation that the core contains little or no RNA, sub-nuclear domains that are known to contain high amounts of RNA, do have high phosphorus signals when imaged by ESI. Structures such as 30 nm chromatin fibres, the nucleolus (Figure 1D), interchromatin granule clusters (Hendzel et al., 1998), or the Sam 68 nuclear bodies (Figure 3, (Chen et al., 1999) have been shown to have high phosphorus content. Because the sensitivity of these procedures has been shown to be very high (Bazett-Jones & Hendzel, 1999; Bazett-Jones et al., 1999), our results rule out

the possibility that the intense staining of these structures using the EDTA-regressive staining method is the result of an abundance of RNA within the structure. Similarly, the nuclear run-on experiment, which shows labelling of the PML nuclear bodies, has a greater potential for experimental artifacts than does the direct incorporation into RNA through addition of fluorouridine into the tissue culture medium. I present a number of independent methods, which demonstrate an absence of (i) bulk chromatin, (ii) acetylated chromatin, (iii) newly synthesized RNA, or (iv) phosphorus-rich nucleic acids, in the core of the PML nuclear body. I conclude, therefore, that it is highly unlikely that the PML nuclear body represents a higher-order nuclear structure that nucleates or aggregates around specific clusters of transcriptionally active genes or even single, highly active genes. Instead, the presence of transcription regulatory factors within the PML nuclear body and the shell of highly acetylated chromatin and nascent RNAs in the immediate vicinity of the PML nuclear body, implicate its role as a driving force in creating or establishing the transcriptional domain. Moreover, it has been recently demonstrated that the hypophosphorylated form of RNA polymerase II is present in some PML nuclear bodies (von Mikecz *et al.*, 2000). This form of RNA polymerase II is involved in the assembly of the transcription machinery at the promoter (Vincent et al., 1996). The presence of CBP and RNA polymerase II provide evidence for a spatial link between coactivators of transcription and the basal transcription machinery in discrete, transcriptionally active nuclear domain. A nuclear-neighbour hypothesis for regulation of nuclear events has been presented to explain a number of similar relationships involving sub-nuclear domains (Schul et al., 1998).

It is possible to overlay a net phoshorus image onto a net nitrogen background image using a blending that allows the phosphorus to become green only when the signal is high for both nitrogen and phosphorus (figure 7A). This green signal will represent the chromatin blocks since it is the only component that has high nitrogen and phosphorus content (RNA fibers being too small and

dispersed to be represented as blocks of phosphorus signal). The remaining grey signal is low in phosphorus and high in nitrogen and represents protein structures (figure 7A). It is then possible to blur the image to lower the resolution to a similar resolution seen by immunofluorescence in order to compare the different structure seen at the ultrastructural level (figure 7A) with the labeling seen by immunofluorescence (figure 7B). This is not correlative microscopy and, therefore, the different images can not be superimposed. However, these images serve to illustrate a model to show that PML nuclear bodies are surrounded by blocks of chromatin (figure 7A) as seen by electron microscopy. Moreover, it is possible to detect highly acetylated chromatin at the periphery of the PML nuclear bodies, as seen by immunofluorescence (figure 7B). Blurring of figure 5 shows that there are elongated fibers coming out of PML nuclear bodies (figure 7C). By comparing this figure to a magnification of figure 6O, where nascent RNA has been pulse-labeled with fluorouridine, it shows that those fibers in figure 7C may very well represent nascent RNA. The model presented of the PML nuclear body is that it is a protein-based structure, surrounded by blocks of highly acetylated chromatin and where nascent RNA is present at the periphery of the PML nuclear body.

Figure 7 Model of the PML nuclear body

A net phosphorus image was overlaid onto a net nitrogen image using a blending that shows in green only regions that have both high nitrogen and phosphorus content (A). This green signal will represent the chromatin blocks since it is the only component that has both high nitrogen and phosphorus content (RNA fibers being too small and dispersed to be represented as blocks of phosphorus signal). The remaining grey signal is low in phosphorus and high in nitrogen and represents protein structures (A). It is then possible to blur the image to lower the resolution to a similar resolution seen by immunofluorescence in order to compare the different structures seen at the ultrastructural level (A) with the labeling seen by immunofluorescence (B). Blurring of Figure 5 shows that there are elongated fibers coming out of PML nuclear bodies (C). By comparing this figure to a magnification of figure 6O, where nascent RNA has been pulse-labeled with fluorouridine, it shows that those fibers in (C) may very well represent nascent RNA.

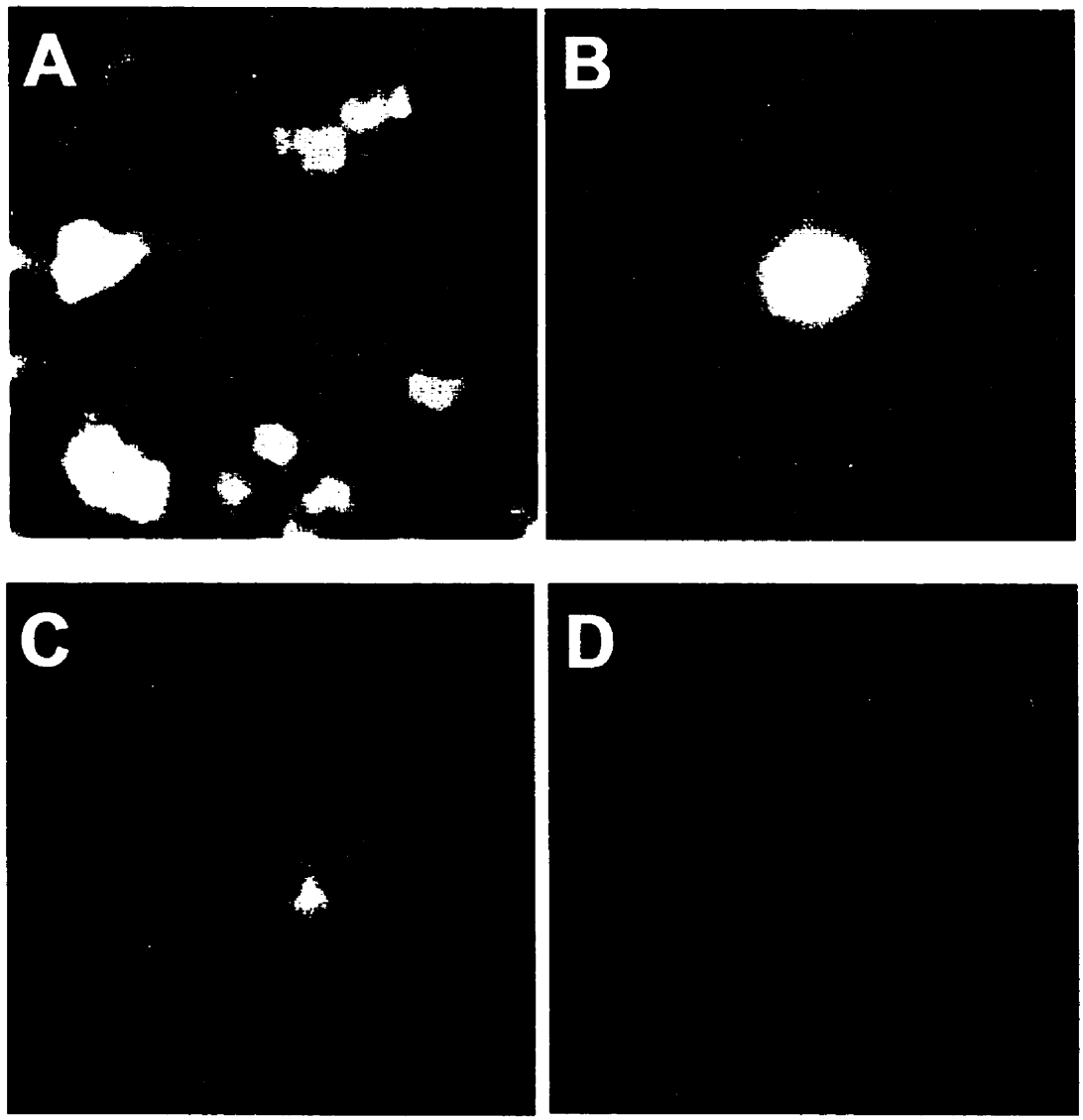
A
B
C
D

Chapter II : The PML nuclear body is a dynamic nuclear structure.

Overview

The cell nucleus is highly organized and contains well-defined sub-domains. In contrast to cytoplasmic organelles, the different sub-nuclear compartments are not separated from the surrounding by a lipid bilayer. Instead, sub-nuclear structures are delineated by an accumulation of specific proteins within a defined volume, and retain a typical size, shape and number under normal growth conditions. It is not known how such compartments are formed and it remains to be shown whether an underlying structural framework locally concentrates the components or whether the local accumulation results from random aggregations of rapidly diffusing components (Phair & Misteli, 2000). Specific proteins have been shown to associate and dissociate rapidly between the nucleoplasm and sub-nuclear compartments (Kruhlak et al., 2000; Phair & Misteli, 2000); how such mobile proteins are concentrated within these compartments is not known.

We have shown that nuclei that have not been exposed to extraction or other disruptive procedures possess a protein-based architecture (Hendzel et al., 1999). Surprisingly, such structures, which are completely devoid of nucleic acid, can be enriched in transcription regulatory factors (Hendzel et al., 1998). The core of the PML nuclear body is an example (Boisvert et al., 2000). Whether these domains represent aggregations of randomly diffusing proteins, or are established by an underlying protein-based architecture, remains to be determined. In this chapter, I show that some components of the PML body are immobile, and may play a structural role, whereas at least one other component, CBP, diffuses into and out of the PML body and accumulates in the PML body under some conditions.

The presence of CBP in PML nuclear bodies is cell line dependent

The transcription co-activator CBP is a component of all PML nuclear bodies in Hep-2 cells (LaMorte et al., 1998) and SK-N-SH cells as detected by immuno-fluorescence microscopy (Boisvert et al., 2000) (Figure 8A, F, K, P). We have found, however, that not all cell lines exhibit this property. For example, HeLa and 293 (Figure 8Q) cells do not concentrate CBP in PML nuclear bodies. When 293 cells are transiently transfected with an expression construct coding for a GFP-CBP fusion protein, the fusion protein is targeted to PML nuclear bodies as well as being distributed throughout the nucleoplasm (Figure 8J). These are cells that do not normally concentrate CBP in PML nuclear bodies. Furthermore, expression of GFP-PML (Figure 8C, H, M, R) also leads to the accumulation of the endogenous CBP in PML nuclear bodies of these cells (293) (Figure 1R). Over-expression of Sp100 in these cells, however, does not bring the endogenous CBP into PML nuclear bodies (Figure 8D, I, N, S). This shows that the presence of CBP within PML nuclear bodies depends on PML, but not Sp100. Interestingly, expression of Sp100 and PML increase the number of PML nuclear bodies in the cells (Figure 8H, I), whereas expression of CBP does not. This indicates that PML and Sp100, but not CBP, participate in the formation of this nuclear structure. CBP is rather concentrated in the existing PML nuclear bodies.

Screening Cell Lines for the Presence of CBP in PML Nuclear Bodies

To determine if CBP was a component of PML nuclear bodies in a majority of cell lines, or if this was characteristic of only a few cell lines, I have screened several cell lines that were available. Using the antibody recognizing the N-terminus of CBP and the antibody recognizing PML, I have co-labeled different cell lines for analysis by immunofluorescence microscopy. I also gathered as much information on each cell line, to determine if the presence of CBP within PML nuclear bodies might be dependent on transformation or presence of viral proteins, or any other common characteristic of the cells. As shown in Table 1, only four cell lines have been found to be enriched for CBP in PML nuclear bodies. These cell

lines are SK-N-SH, CHO, COS1 and Hep-2. The presence of CBP in Hep-2 cells could not be detected by the antibody against the N-terminus of CBP, but has been shown by another group (LaMorte et al., 1998). The fact that we cannot detect CBP in PML nuclear bodies in some cell lines implies that the epitope is masked or modified in those cells. The presence of CBP in PML nuclear bodies does not depend on the transformation state of the cell lines, since CHO cells (Chinese Hamster Ovary), which are not transformed, can enrich CBP in PML nuclear bodies (see table 1). Presence or absence of viral proteins does not prevent CBP from enriching in PML nuclear bodies, since COS-1, which are positive for the large T antigen of SV40 virus, still show CBP in PML nuclear bodies (table 1).

FRAP analysis of GFP-CBP movement

To determine whether CBP is a mobile molecule in the nucleus, and moves in or out of PML nuclear bodies, we measured its mobility using the technique fluorescence recovery after photo-bleaching (FRAP). The approach uses a high intensity laser from a laser scanning microscope to irreversibly bleach half of a nucleus of a cell expressing a GFP fusion protein (boxes in Figure 9 represent the bleached region). Following photobleaching, the cell is imaged at different times to follow the redistribution of the unbleached GFP fusion proteins. Because the bleaching process irreversibly eliminates fluorescence of the GFP without affecting the rest of the protein, it is possible to visualise the normal movement of the unbleached protein in the cell. The recovery of the fluorescence is a measure for the mobility of the protein.

Transient expression of GFP-CBP shows two different populations of the fusion proteins, one that is concentrated in PML nuclear bodies and one that is dispersed throughout the nucleus (Figure 9C, Figure 8H). The GFP-CBP observed outside of PML nuclear bodies, dispersed throughout the cell nucleus, moves more than 50 times slower than GFP alone (Figure 10E, G). This difference in mobility is

likely not a consequence of the size of the protein, rather is due to interaction with other nuclear components (Kruhlak et al., 2000; Phair & Misteli, 2000; Seksek *et al.*, 1997). Fluorescence recovery of these proteins is significantly faster than GFP-histone H2B which is immobile over very long periods of time (4h) ((Phair & Misteli, 2000); my own observations). A time period of 7.5 minutes was necessary for the GFP-CBP signal to reach equilibrium with the bleached half of the nucleus compared to only 14 seconds for the GFP protein alone. The half-recovery time was calculated to be 92 seconds and 1.8 seconds respectively for GFP-CBP and GFP alone. There was no apparent difference in rates of recovery between CBP in PML nuclear bodies and the CBP population that is dispersed throughout the nucleoplasm (Figure 9C). This means that GFP-CBP is capable of moving into and out of PML nuclear bodies very rapidly, and so is not permanently bound inside PML nuclear bodies. In control experiments, in which the entire nuclear fluorescence was bleached, recovery was not observed over long time periods, indicating that *de novo* synthesis, import of a cytoplasmic pool, or refolding of the GFP molecule did not contribute significantly to fluorescence recovery (data not shown). Moreover, cells can be bleached several times and will still show similar kinetics of recovery, indicating that there is no immediate damage induced by scanning the cell using high intensity 488 nm wavelength light. We have also shown that paraformaldehyde-fixed cells show no recovery after photobleaching.

CBP exchange rate with PML nuclear bodies is rapid and bi-directional

The rate of fluorescence recovery of CBP in PML nuclear bodies is equivalent to that found in the nucleoplasm. To determine whether the direction of CBP movement is only into PML nuclear bodies or is bi-directional, into and out of PML nuclear bodies, we performed both FRAP and fluorescence loss in photo-bleaching (FLIP) experiments. To determine the rate of movement from the nucleoplasm into PML nuclear bodies, we bleached an entire PML nuclear body in a cell expressing GFP-CBP (Figure 11A). Complete fluorescence recovery of the

PML nuclear body was observed after 5 sec. This indicates that CBP can move rapidly from the nucleoplasm into PML nuclear bodies. To determine whether CBP can leave the PML nuclear body, we bleached a region just outside the PML nuclear body to see whether we could drain some fluorescence from the PML nuclear body (FLIP) (Figure 11B). Indeed, we observed a loss of fluorescence from the PML nuclear body followed by a quick re-equilibration (5 seconds) of the fluorescence. Therefore, we conclude that the movement of GFP-CBP between the nucleoplasm and the PML nuclear bodies is rapid and bi-directional. These experiments indicate that CBP in PML nuclear bodies is not an insoluble aggregation of molecules, which form by random clustering of diffusing molecules. Instead, CBP can associate and dissociate rapidly, into and out of these domains. These results further demonstrate that CBP molecules are not recruited to these domains and then degraded (Maul, 1998).

FRAP analysis of GFP-PML and GFP-Sp100 movement

In contrast to the rate of movement of GFP-CBP in live cells, GFP-PML (Figure 9A) and GFP-Sp100 (Figure 9B) fluorescence recovery occurred over much longer times and showing very little recovery even after 10 minutes, indicating that these molecules are stationary and immobile. The estimated time for full recovery was 77 and 92 minutes for GFP-PML and GFP-Sp100, respectively. This indicates that PML and Sp100 are not local concentrations of protein that form through stochastic aggregation events from randomly diffusing molecules. Instead, the dynamic properties of Sp100 and PML are consistent with structural proteins that contribute to the integrity of the PML nuclear body, which we propose, is a specialised component of the protein-based nuclear architecture.

Sp100 and PML are also immobile inside the PML nuclear bodies

If Sp100 and PML play a structural role, we would predict that they would also be immobile within the PML nuclear body itself. To determine whether GFP-

Sp100 is moving within the PML nuclear body, we performed FRAP at high resolution, bleaching a line passing through the middle of a single PML nuclear body (Figure 12A). We found that the fluorescence within the PML nuclear body only recovers after relatively long periods (4 minutes). The same result was obtained for PML within PML nuclear bodies (data not shown). In contrast, GFP-CBP (Figure 12B) fluorescence recovers quickly from such a treatment, making it difficult to observe the bleached line inside the PML nuclear body in the first image recorded after the bleaching step. After 5 seconds, the fluorescence of GFP-CBP has completely been redistributed throughout the PML nuclear bodies. The rate of redistribution is greater than that observed when a half nucleus is bleached, because the distance that the proteins have to travel is comparatively much less. Again, the lack of movement of Sp100 and PML within the PML nuclear bodies lead us to conclude that they play a structural role in these domains, and they are not aggregates maintained by randomly diffusing molecules.

Figure 8 Presence of CBP in PML Nuclear Bodies is Cell Line Depend

Co-localization of CBP and PML proteins in SK-N-SH cells (A, F, K, and P) but not in 293 cells (B, G, L, Q). Overexpression of GFP-PML in 293 cells (C, H) allows proper targeting into PML bodies (C) and concentrate CBP inside the structure (M, R). However, overexpression of GFP-Sp100 in 293 cells (D, I) does not concentrate CBP in PML bodies (N, S). Overexpression of GFP-CBP in 293 cells (E, J) targets this protein within PML bodies (O, T). Scale bar represents 5 um.

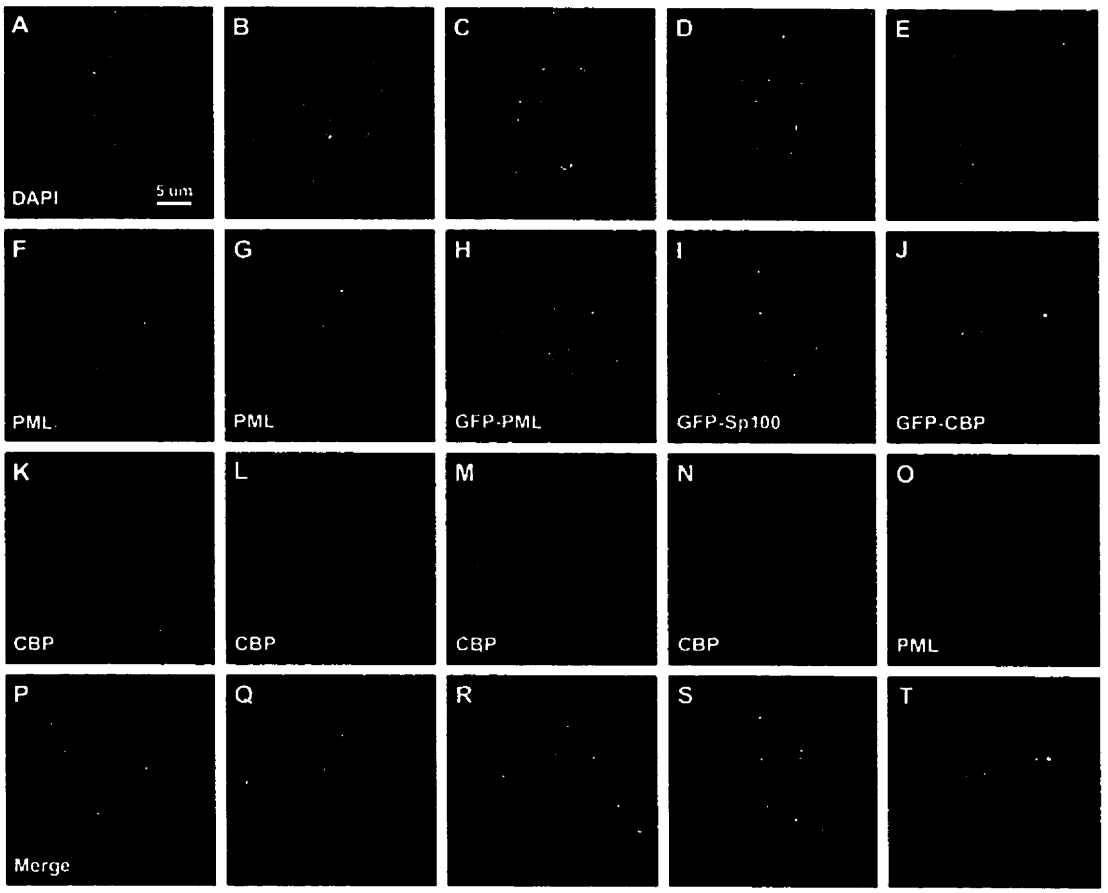
A
DAPI
5 um
B
C
D
E
F
PML
G
PML
H
GFP-PML
I
GFP-Sp100
J
GFP-CBP
K
CBP
L
CBP
M
CBP
N
CBP
O
PML
P
Merge
Q
R
S
T

Table I Screening of Cell Lines for the Presence of CBP in PML Nuclear Bodies

Different cell lines were labeled for immunofluorescence microscopy using an anti-PML antibody and an anti-CBP antibody recognizing the N-terminus of the protein. The cells were then observed to determine the presence of CBP within the PML nuclear bodies. The information was put in a table along with the transformation state of the cell lines and the presence of viruses.

Cell	Species	Transformed	Infected	PML	CBP	Other
Sk-N-SH	Human	Yes	No	Yes	Yes	Neuroblastoma
HEp-2	Human	Yes	No	Yes	Yes	Larynx Carcinoma
CHO	Chinese Hamster	No	No	Yes	Yes	Ovary
HeLa	Human	Yes	Yes (Papilloma)	Yes	No	Cervix Carcinoma
Hs68	Human	No	No	Yes	No	foreskin fibroblast
Rat1	Rat	?	?	Yes	No	From R.Johnston
Balb/c 3T3	Mouse	No	No	No	No	
293	Human	Yes	No	Yes	No	
293T	Human	Yes	Yes	Yes	No	
NIH 3T3	Mouse	No	No	No	No	
COS-1	African Monkey	Yes	Yes (SV40)	Yes	Yes	Large T antigen
IM	Indian Muntjac	No	No	No	No	
HEp-G2	Human	Yes	No	Yes	No	Hepatocarcinoma

Figure 9 FRAP of Cells Expressing GFP-PML, GFP-Sp100 or GFP-CBP.

FRAP of a half-nucleus of cells expressing GFP-PML (A), GFP-Sp100 (B) or GFP-CBP (C). Cells were first imaged before the bleaching (Pre-Bleached). Cells where then bleached by scanning a region corresponding to half the nucleus (white boxes) 100 times with the laser at 25% of its maximal intensity. An image was recorded immediately after the bleaching (Bleached, time = 0sec). The mobility of the GFP-tagged proteins was studied by following the redistribution of the fluorescence over time. Each time point is indicated at the bottom right of each image.

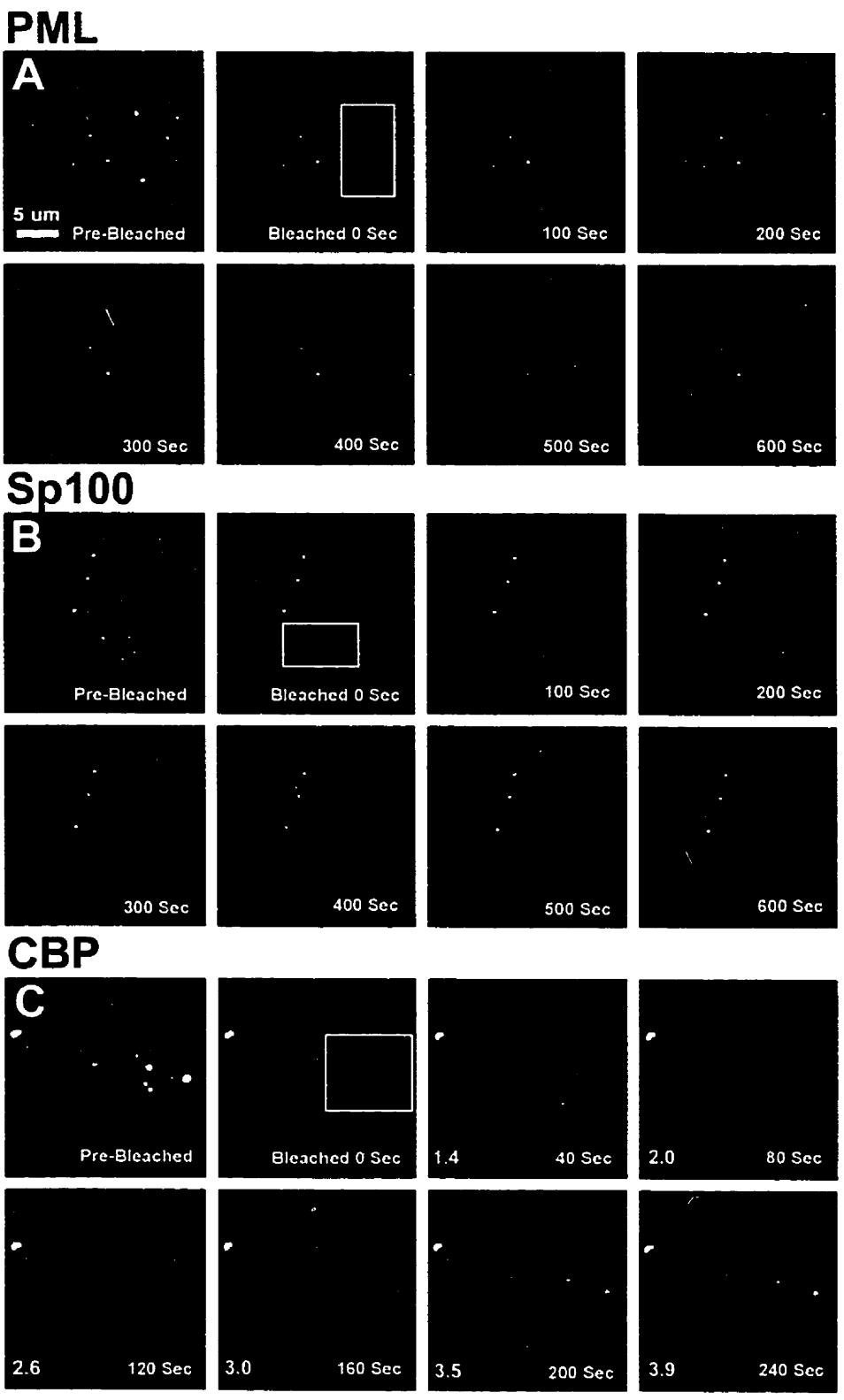
PML
A
5 um
Pre-Bleached
Bleached 0 Sec
100 Sec
200 Sec
300 Sec
400 Sec
500 Sec
600 Sec
Sp100
B
Pre-Bleached
Bleached 0 Sec
100 Sec
200 Sec
300 Sec
400 Sec
500 Sec
600 Sec
CBP
C
Pre-Bleached
Bleached 0 Sec
1.4
40 Sec
2.0
80 Sec
2.6
120 Sec
3.0
160 Sec
3.5
200 Sec
3.9
240 Sec

Figure 10 Recovery Curves Showing the Kinetics of Redistribution of GFP-CBP, GFP-PML and GFP-Sp100

The fluorescence intensity in the bleached and the unbleached region was measured and expressed as a relative intensity, where a value of 1 is equal intensity on both half. This relative intensity was then plotted over time. Recovery curves for CBP (D), PML (E), Sp100 (F) shows kinetics of redistribution of the different fluorescent proteins following bleaching. As control, recovery of GFP alone was measured (G).

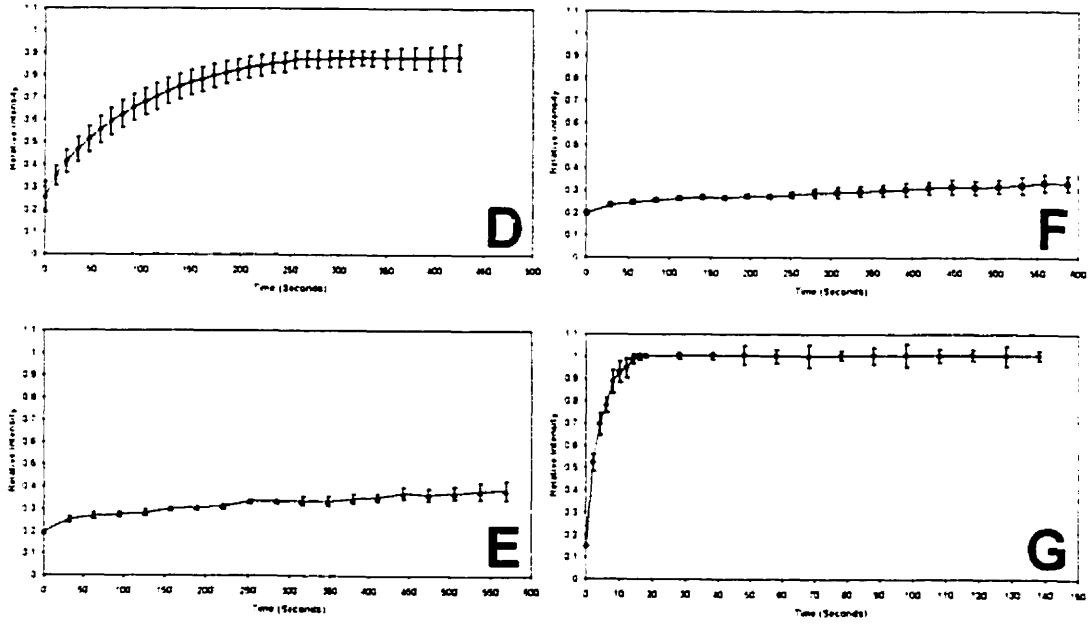
D
F
E
G

Figure 11 Determination of the direction of movement of GFP-CBP.

Bleaching of a whole PML nuclear body (B, box) of a cell expressing GFP-CBP shows a quick recovery (5 seconds, C) of the fluorescence, indicating that CBP travel from the nucleoplasm to the PML nuclear body very fast. Bleaching a region just outside the PML nuclear body (E, box) indicate that we can drain some fluorescence from the PML nuclear body (E) followed by a quick re-equilibration (5 seconds, F) of the fluorescence. Scale bar 300 nm.

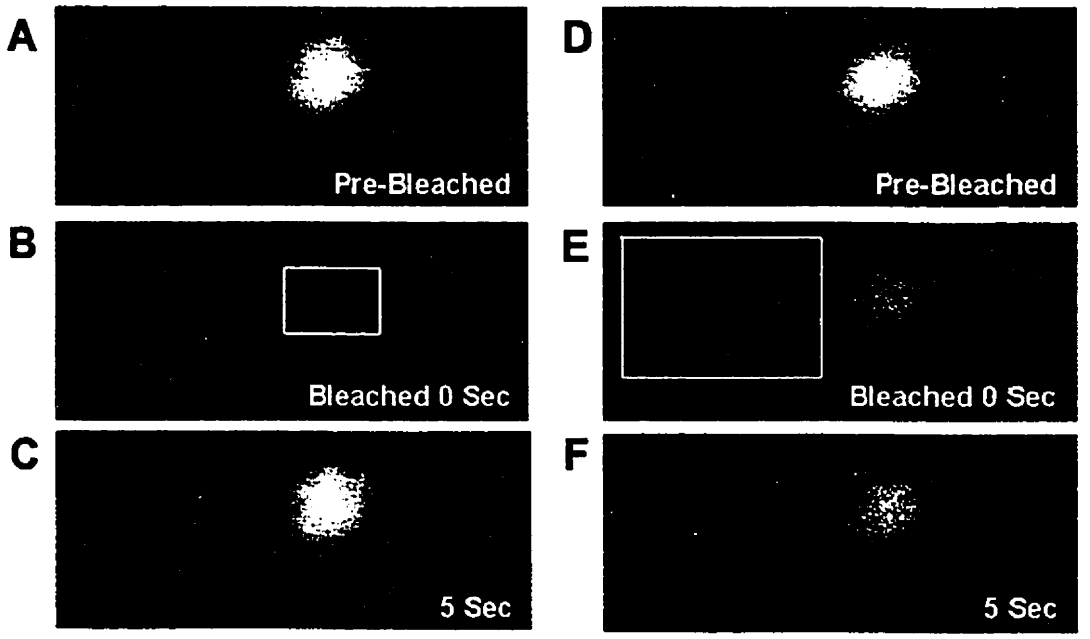
A
Pre-Bleached
B
Bleached 0 Sec
C
5 Sec
D
Pre-Bleached
E
Bleached 0 Sec
F
5 Sec

Figure 12 FRAP of Subregions of PML Nuclear Bodies Expressing GFP-Sp100 and GFP-CBP.

I bleached a line going through the middle of one PML nuclear body (see boxes) from cells expressing GFP-Sp100 (A) and GFP-CBP (B). We have found that the fluorescence does not move and recovers very slowly over the line for GFP-Sp100 for relatively long periods (270 seconds). However, GFP-CBP (Figure B) recovers so fast from such a treatment that it is almost impossible to see the bleached line inside the PML nuclear bodies. After 5 seconds, the fluorescence of GFP-CBP has completely been redistributed throughout the PML nuclear bodies. Bleached boxes are approximately 300 nm in length.

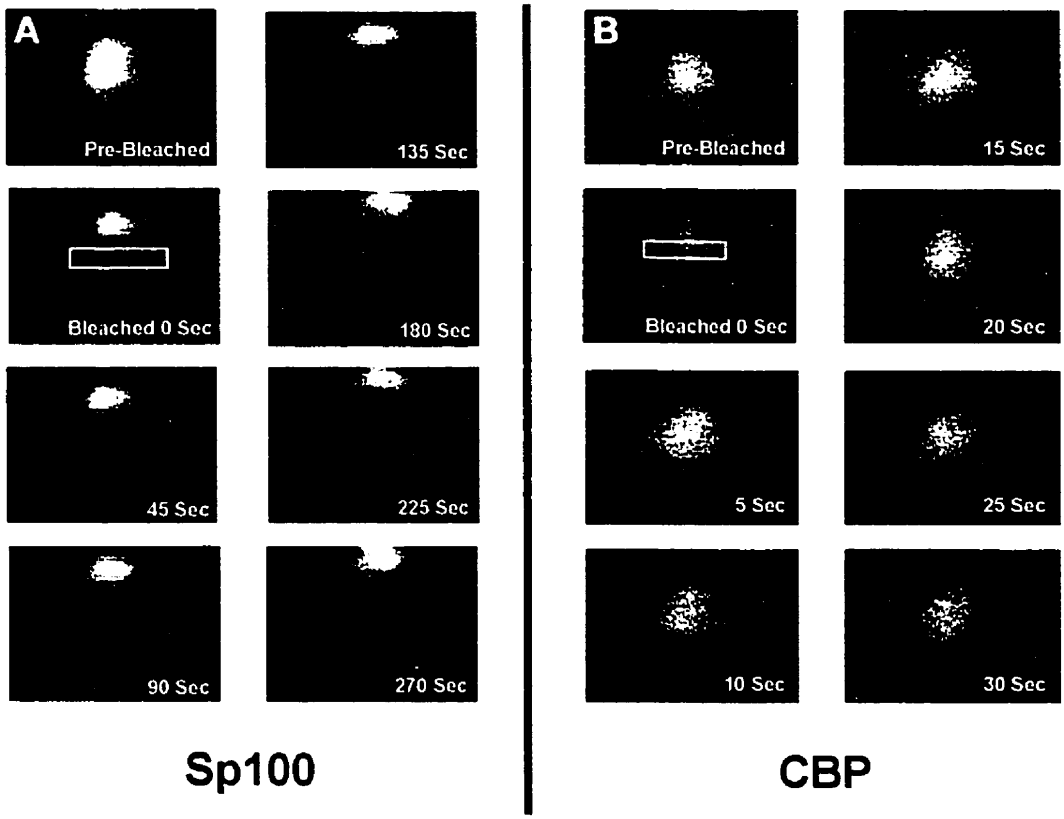
A
Pre-Bleached
135 Sec
Bleached 0 Sec
180 Sec
45 Sec
225 Sec
90 Sec
270 Sec
Sp100
B
Pre-Bleached
15 Sec
Bleached 0 Sec
20 Sec
5 Sec
25 Sec
10 Sec
30 Sec
CBP

Discussion

Several different proteins have the potential to localize to varying degrees within these sub-nuclear domains, including PML and Sp100, which are consistently found there. CBP, on the other hand, is concentrated in PML nuclear bodies only under certain conditions. For example, there are many cell lines where immunofluorescence microscopy cannot detect an accumulation of CBP in PML nuclear bodies. However, even the lowest levels of over-expression of PML or CBP above the endogenous levels in these cells can lead to an accumulation of CBP in these domains. One model for the formation of such protein enrichments in the nucleoplasm is based on stochastic interactions of rapidly diffusing molecules (Phair & Misteli, 2000). This model may accurately apply to the formation of some sub-nuclear domains, but apparently does not apply to PML nuclear bodies. At least two components of PML nuclear bodies, PML itself and Sp100 are not freely diffusing proteins in the nucleoplasm. They represent nuclear proteins that are tightly bound to these domains, and do not move significantly even within individual bodies. Therefore, these two proteins are likely to be structural, like a framework for the PML nuclear body.

In contrast, CBP moves relatively rapidly into and out of these domains, although significantly slower than GFP, a protein that would not be expected to bind specifically to any sub-nuclear complexes. Therefore, there appear to be sites throughout the nucleoplasm with which CBP can interact, but discrete domains where the in rate is sufficiently higher than the out rate, leading to accumulation. The observation that CBP is a component of PML nuclear bodies in some cell lines, or can be forced to accumulate in PML nuclear bodies with even low levels of over-expression of Pml or CBP itself, indicates that CBP may transit through PML nuclear bodies, and accumulate there if the "in rate" is higher than the "out rate". The steady state levels of CBP in PML nuclear bodies, therefore, could be shifted with slight changes in concentration of factors with which CBP interacts.

I propose that PML acts as an anchor for concentrating factors such as CBP, which are diffusing at a moderate rate. The local accumulation of CBP, a transcriptional co-activator and histone acetyltransferase, may create a domain on the periphery of PML nuclear bodies that is enriched in acetylated and transcriptionally active chromatin. Indeed, I have observed that the chromatin surrounding PML nuclear bodies is acetylated and nascent RNA is associated with the periphery of these domains (Chapter 1) (Boisvert et al., 2000). Hence, biochemical alteration of the domain, by altering composition or physical integrity, may lead to aberrant gene regulation and a transformed phenotype (Zhong et al., 2000a).

Conclusion

There has been an increasing interest in the PML nuclear bodies in the past few years because of their involvement in viral infection (Maul, 1998; Sterndorf et al., 1997a; Zhong et al., 2000a) and their disruption and disappearance in acute promyelocytic leukemia (de The et al., 1991; Kakizuka et al., 1991). Whether this structure serves only as a storage site for regulatory factors, functions as a site for transcription by creating a suitable environment, or plays some other role, will only be determined as its structure and composition are characterized. In this study, I have addressed several questions about the structure, organization, function and dynamics properties of the PML nuclear body.

Sub-nuclear compartments that function to concentrate regulatory factors and complexes may be important in modulating gene expression (Schul et al., 1998). The interchromatin granule cluster (IGC), for example, is able to concentrate transcriptional co-activators in the protein-rich core, and is surrounded by transcriptionally active chromatin (Hendzel et al., 1998). Indeed, the periphery of IGCs are sites of transcription of particular genes (Smith *et al.*, 1999). PML nuclear bodies, which, incidentally, are generally associated with IGCs (Ishov et al., 1997), may also serve to concentrate regulatory factors that service transcriptional events on their surfaces.

My model for the PML nuclear body is that the protein core is composed of a protein framework which consists of at least the PML protein and Sp100 (figure 13). This protein structure serves as an anchor to enrich transcriptional regulatory factors, such as CBP, and factors that affect transcription regulation of the gene family that surrounds the core. The consequence of such enrichment is that the surrounding chromatin is highly acetylated and, therefore, has a very high potential for transcription. The genes that are implicated in requiring PML nuclear bodies for expression are early viral genes (Chelbi-Alix et al., 1995; Grotzinger *et al.*, 1996;

Guldner et al., 1992; Ishov et al., 1997; Lavau *et al.*, 1995), and possibly genes important for immune function, including MHC class I and II (Fontes et al., 1999; Kretsovali et al., 1998; Zheng et al., 1998). Like the IGC, the core of the PML nuclear body is protein-rich. The major compositional difference between the two sub-nuclear domains is that the core of the IGC also contains structural RNA and/or pre-mRNA, whereas the core of the PML nuclear body contains no nucleic acid. The fact that viral genomic DNA can be efficiently targeted to the periphery of the PML nuclear bodies indicates that one or more specific DNA sequences are able to target DNA to PML nuclear bodies. It is very likely that some genes have sequences within their promotors that function similarly to the viral sequences. The presence of such sequences in some genes would have the consequence of specifically targeting them to the periphery of the PML nuclear bodies, into a transcriptionally favourable environment.

It is interesting to note that PML regulates p53 acetylation and premature senescence in the presence of oncogenic proteins such as Ras (Pearson *et al.*, 2000). Ras upregulates PML expression, which induces senescence in a p53-dependent manner. At this point, p53 is found in PML nuclear body in a trimeric complex including p53, PML and CBP. CBP can then acetylate p53 at lysine 382, an event that is essential for its biological function (Giacca & Kastan, 1998). Since Ras activates the Elk-1 and the AP-1 (Jun/fos) transcription factors through the MAP kinase pathway, it is possible that the PML promoter is responsive to one or both of these two transcription activators. This finding may shed new light on understanding the treatment of APL through the use of deacetylase inhibitors. It was proposed that the induction of differentiation in the presence of HDAC inhibitors was possibly through the inactivation of HDACs in the RAR pathway (Kitamura et al., 2000). However, it is also possible that deacetylases inhibitors keep p53 in an acetylated state, thus allowing its stability and its activation. This supports the model in which the integrity of the PML nuclear body, and not the RAR transcription pathway, is important for proper differention of promyelocytes.

The fact that PML bodies may serve as a site for modification of proteins implies that they are not only involved in transcriptional processes, but also in other functions that are yet to be discovered.

Figure 13 Model of the PML nuclear body

The PML nuclear body is a protein structure compose of at least the PML protein and Sp100 (grey). This protein backbone serves as an anchor to enrich in transcription factors or activators such as CBP (red). In consequence, the chromatin (blue) surrounding the PML nuclear body is highly acetylated and transcriptionally active (green). This allows the genes targeted at the periphery of the PML nuclear bodies to have a higher rate of transcription.

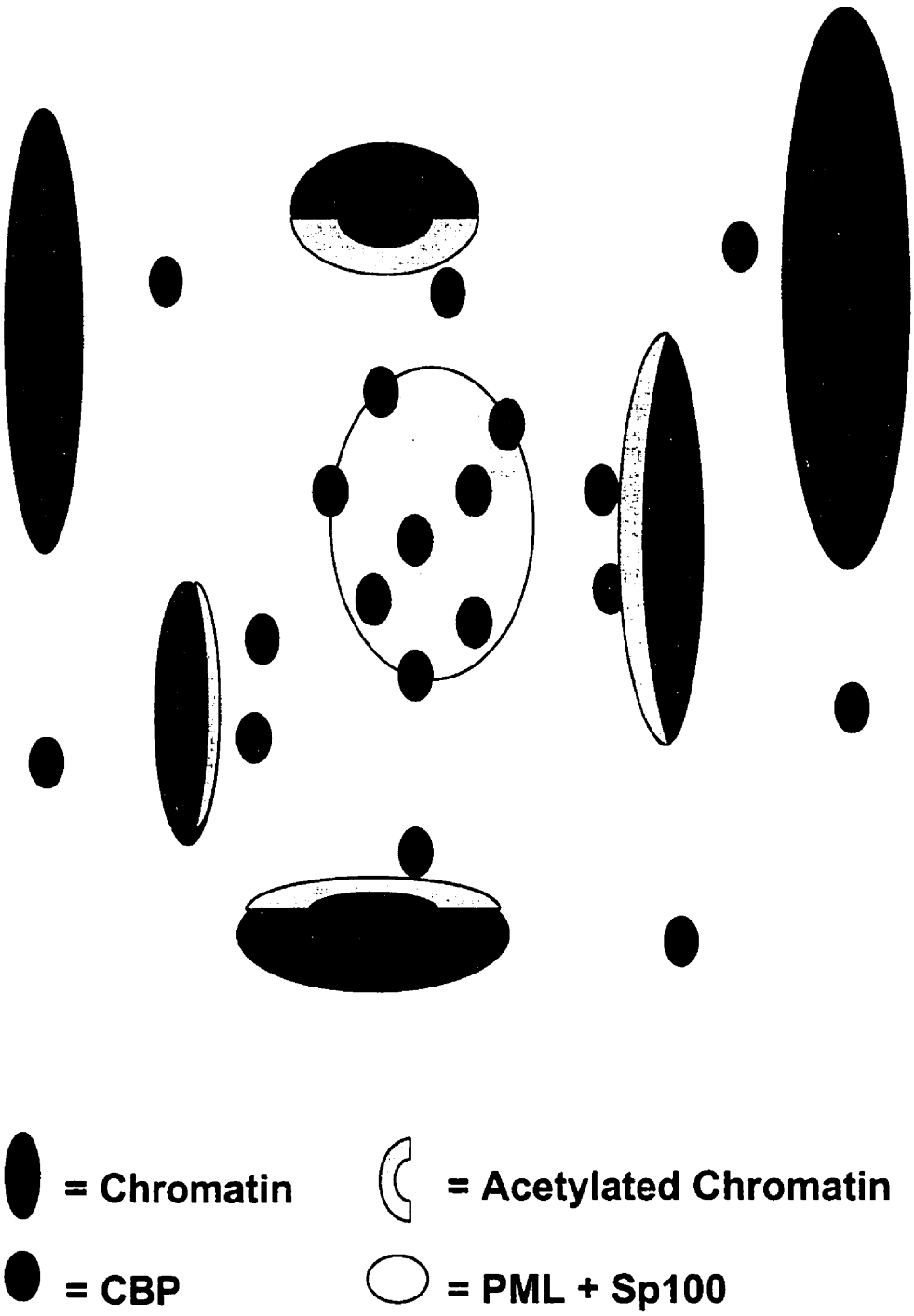
= Chromatin
= Acetylated Chromatin
= CBP
= PML + Sp100

Future Directions

There is much evidence for the involvement of the PML nuclear body in transcription. Obviously only some of the transcription in a nucleus could occur at the periphery of this structure, implying that only a small subset of genes are transcribed there. It would be interesting to determine what particular genes are transcribed around the PML nuclear bodies, and how they are targeted to these sites. It should be possible to identify a DNA sequence that would allow a piece of DNA (like a plasmid) to be targeted to the periphery of the PML nuclear body. A good starting point would be the genome of a DNA virus, like HSV or Ad5, since the DNA alone is sufficient for targeting to the PML nuclear body (Ishov & Maul, 1996). The identification of such a sequence would allow a screening of the human genome to identify genes that have the potential to be targeted to the PML nuclear body.

Another important area for investigation is the effect of HIV-1 infection on PML nuclear bodies. HIV-1 transactivator Tat can disrupt PML nuclear bodies and prevent the PML protein from entering the nucleus (my own observations). Moreover, after HIV-1 infection, the PML nuclear bodies move from the nucleus to the cytoplasm for a short period of time (4-6 hours) and go back to the nucleus (communicated by Dr. E. Verdin, UCSF). However, it is not known why and how HIV-1 affects PML nuclear bodies. A reasonable possibility is that it may involve CBP since Dr. Verdin's group has shown that Tat is specifically acetylated by p300 and CBP.

References

Abney, J. R., Cutler, B., Fillbach, M. L., Axelrod, D. & Scalettar, B. A. (1997). Chromatin dynamics in interphase nuclei and its implications for nuclear structure. *Journal of Cell Biology* **137**(7), 1459-1468.

Ahn, J. H., Brignole, E. J. r. & Hayward, G. S. (1998). Disruption of PML subnuclear domains by the acidic IE1 protein of human cytomegalovirus is mediated through interaction with PML and may modulate a RING finger-dependent cryptic transactivator function of PML. *Molecular and Cellular Biology* **18**(8), 4899-4913.

Alcalay, M., Tomassoni, L., Colombo, E., Stoldt, S., Grignani, F., Fagioli, M., Szekely, L., Helin, K. & Pelicci, P. G. (1998). The promyelocytic leukemia gene product (PML) forms stable complexes with the retinoblastoma protein. *Molecular and Cellular Biology* **18**, 1084-1093.

Alcalay, M., Zangrilli, D. & Pandolfi, P. P. (1991). Translocation breakpoint of acute promyelocytic leukemia lies within the retinoic acid receptor alpha locus. *Proceedings of the National Academy of Science of the USA* **88**, 1977-1981.

Altabef, M., Garcia, M., Lavau, C., Bae, S.-C., Dejean, A. & Samarut, J. (1996). A retrovirus carrying the promyelocyte-retinoic acid receptor PML-RARa fusion gene transforms haematopoietic progenitors in vitro and induces acute leukemias. *EMBO Journal* **15**, 2707-2718.

Arany, Z., Newsome, D., Oldread, E., Livingston, D. M. & Eckner, R. (1995). A family of transcriptional adaptor proteins targeted by the E1A oncoprotein. *Nature* **374**(6517), 81-84.

Ascoli, C. A. & Maul, G. G. (1991). Identification of a novel nuclear domain. *Journal of Cell Biology* **112**, 785-795.

Bazett-Jones, D. P. & Hendzel, M. J. (1999). Electron spectroscopic imaging of chromatin. *Methods: A Companion to Methods in Enzymology* **17**, 1888-200.

Bazett-Jones, D. P., Hendzel, M. J. & Kruhlak, M. J. (1999). Stoichiometric analysis of protein- and nucleic acid-based structures in the cell nucleus. *Micron*.

Bernhard, W. (1969). A new staining procedure for electron microscopical cytology. *Journal of Ultrastructural Research* **27**, 250-265.

Bernstein, R. M., Neuberger, J. M., Bunn, C. C., Callender, M. E., Hughes, G. R. & Williams, R. (1984). Diversity of autoantibodies in primary biliary cirrhosis and chronic active hepatitis. *Clinical Experimental Immunology* **55**, 553-560.

Boddy, M. N., Howe, K., Etkin, L. D., Solomon, E. & Freemont, P. S. (1996). PIC-1, a novel ubiquitin-like protein which interacts with the PML component of a multiprotein complex that is disrupted in acute promyelocytic leukemia. *Oncogene* **13**(5), 971-982.

Boggs, B. A., Connors, B., Sobel, R. E., Chinaud, A. C. & Allis, C. D. (1996). Reduced levels of histone acetylation on the inactive X chromosomes as shown by histone acetylation. *Chromosoma* **105**, 41-49.

Boisvert, F.-M., Hendzel, M. J. & Bazett-Jones, D. P. (2000). Promyelocytic Leukemia (PML) Nuclear Bodies are protein structures that do not accumulate RNA. *Journal of Cell Biology* **148**(2), 282-292.

Borden, K. L. (2000). RING domains: master builders of molecular scaffolds? *Journal of Molecular Biology* **295**(5), 1103-1112.

Borden, K. L., CampbellDwyer, E. J. & Salvato, M. S. (1997). The promyelocytic leukemia protein PML has a pro-apoptotic activity mediated through its RING domain. *FEBS Letter* **418**((1-2)), 30-34.

Borden, K. L., Lally, J. M., Martin, S. R., O'Reilly, N. J., Solomon, E. & Freemont, P. S. (1996). In vivo and in vitro characterization of the B1 and B2 zinc-binding domains from the acute promyelocytic leukemia protooncoprotein PML. *Proc Natl Acad Sci U S A* **93**(4), 1601-1606.

Borrow, J., Goddard, A. D., Sheer, D. & Solomon, E. (1990). Molecular analysis of acute promyelocytic leukemia breakpoint cluster region on chromosome 17. *Science* **249**, 1577-1580.

Breitman, T. R., Selonick, S. E. & Collins, S. J. (1980). Induction of differentiation of the human promyelocytic leukemia cell line (HL-60) by retinoic acid. *Proceedings of the National Academy of Science of the USA* **77**, 2936-2940.

Campbell Dwyer, E. J., Lai, H., MacDonald, R. C., Salvato, M. S. & Borden, K. L. (2000). The lymphocytic choriomeningitis virus RING protein Z associates with eukaryotic initiation factor 4E and selectively represses translation in a RING-dependent manner. *Journal of Virology* **74**(7), 3293-3300.

Chang, K. S., Fan, Y.-H., Andreeff, M., Liu, J. & Mu, Z.-M. (1995). The PML gene encodes a phosphoprotein associated with the nuclear matrix. *Blood* **85**, 3646-4653.

Chelbi-Alix, M. K., Pelicano, L., Quignon, F., Koken, M. H. M., Venturini, L., Stadler, M., Pavlovic, J., Degos, L. & de The, H. (1995). Induction of the PML protein by interferons in normal and APL cells. *Leukemia* **9**, 2027-2033.

Chen, T., Boisvert, F. M., Bazett-Jones, D. P. & Richard, S. (1999). A role for the GSG domain in localizing Sam68 to novel nuclear structures in cancer cell lines. *Molecular Biology of the Cell* **10**(9), 3015-3033.

De Bruyn-Kops, A. & Knipe, D. M. (1994). Preexisting nuclear architecture defines the intranuclear location of herpes virus DNA replication structures. *Journal of Virology* **68**(3512-3526).

De Graaf, A., Humbel, B. M., Stuurman, N., van Bergen en Henegouwen, P. M. P. & Verkleij, A. J. (1992). Three-dimensional immunogold labeling of nuclear matrix proteins in permeabilized cells. *Cell Biology International Reports* **16**, 827-836.

de The, H., Chomienne, C., Lanotte, M., Degos, L. & Dejean, A. (1990). The t(15;17) translocation of acute promyelocytic leukaemia fuses the retinoic acid receptor alpha gene to a novel transcribed locus. *Nature* **347**, 558-561.

de The, H., Lavau, C., Marchio, A., Chomienne, C., Degos, L. & Dejean, A. (1991). The PML-RAR alpha fusion mRNA generated by the t(15;17) translocation in acute promyelocytic leukemia encodes a functionally altered RAR. *Cell* **66**, 675-684.

Del Sal, G., Manfioletti, G. & Schneider, C. (1989). The CTAB-DNA precipitation method: a common mini-scale preparation of template DNA from phagemids, phages or plasmids suitable for sequencing. *Biotechnique* **7**(5), 514-520.

Desbois, C., Rousset, R., Bantignies, F. & Jalinot, P. (1996). Exclusion of Int-6 from PML nuclear bodies by binding to the HTLV-1 Tax oncoprotein. *Science* **273**, 951-953.

Doucas, V., Ishov, A. M., Romo, A., Juguilon, H., Weitzman, M. D., Evans, R. M. & Maul, G. G. (1996). Adenovirus replication is coupled with the dynamic properties of the PML nuclear structure. *Genes & Development* **10**, 196-207.

Doucas, V., Tini, M., Egan, D. A. & Evans, R. M. (1999). Modulation of CREB binding protein function by the promyelocytic (PML) oncoprotein suggests a role for nuclear bodies in hormonbe signaling. *Proceedings of the National Academy of Science of the USA* **96**, 2627-2632.

Duprez, E., Lillehaug, J. R., Naoe, T. & Lanotte, M. (1996). cAMP signalling is decisive for recovery of nuclear bodies (PODs) during maturation of RA-resistant t(15;17) promyelocytic leukemia NB4 cells expressing PML-RAR alpha. *Oncogene* **12**(11), 2451-2459.

Duprez, E., Saurin, J. M., Desterro, J. M., Lallemand-Breitenbach, V., Howe, K., Boddy, M. N., Solomon, E., de The, H., Hay, R. T. & Freemont, P. S. (1999). SUMO-1 modification of the acute promyelocytic leukaemia protein PML: implications for nuclear localisation. *Journal of Cell Science* **112**, 381-393.

Dyck, J. A., Maul, G. G., Miller, W. H. J., Chen, J. D., Kakizuka, A. & Evans, R. M. (1994). A novel macromolecular structure is a target of the promyelocytic-retinoic acid receptor oncoprotein. *Cell* **76**(333-343).

Everett, R. D., Freemont, P., Saitoh, H., Dasso, M., Orr, A., Kathoria, M. & Parkinson, J. (1998). The disruption of ND10 during herpes simplex virus infection correlates with the Vmw110- and proteasome-dependent loss of several PML isoforms. *Journal of Virology* **72**(8), 6581-6591.

Everett, R. D. & Maul, G. G. (1994). HSV-1 IE protein Vmw110 causes redistribution of PML. *EMBO Journal* **13**(21), 5062-5069.

Everett, R. D., Meredith, M. & Orr, A. (1999). The ability of herpes simplex virus type 1 immediate-early protein Vmw110 to bind to a ubiquitin-specific protease contributes to its roles in the activation of gene expression and stimulation of virus replication. *Journal of Virology* **73**(1), 417-426.

Everett, R. D., Meredith, M., Orr, A., Cross, A., Kathoria, M. & Parkinson, J. (1997). A novel ubiquitin-specific protease is dynamically associated with the PML nuclear domain and binds to a herpesvirus regulatory protein. *EMBO Journal* **16**(3), 566-577.

Fagioli, M., Alcalay, M., Pandolfi, P. P., Venturini, L., Mencarelli, A., Simeone, A., Acampora, D., Grignani, F. & Pelicci, P. G. (1992). Alternative splicing of PML transcripts predicts coexpression of several carboxy-terminally different protein isoforms. *Oncogene* **7**(6), 1083-1091.

Fagioli, M., Alcalay, M., Tomassoni, L., Ferrucci, P. F., Mencarelli, A., Riganelli, D., Grignani, F., Pozzan, T., Nicoletti, I., Grignani, F. & Pelicci, P. G. (1998). Cooperation between the RING + B1-B2 and coiled-coil domains of PML is necessary for its effects on cell survival. *Oncogene* **16**(2905-2913).

Fejes-Toth, G., Pearce, D. & Naray-Fejes-Toth, A. (1998). Subcellular localization of mineralocorticoid receptors in living cells: effects of receptor agonists and antagonists. *Proceedings of the National Academy of Science of the USA* **95**(6), 2973-2978.

Ferrucci, P. F., Grignagi, F., Pearson, M., Fagioli, M., Nicoletti, I. & Pelicci, P. G. (1997). Cell death induction by the acute promyelocytic leukemia-specific PML/RARa fusion protein. *Proceedings of the National Academy of Science of the USA* **94**, 10901-10906.

Flavell, R. A., Allen, H., Burkly, L. C., Sherman, D. H., Waneck, G. L. & Widera, G. (1986). Molecular Biology of the H-2 histocompatibility complex. *Science* **233**, 437-439.

Flynn, P. J., Miller, W. J., Weisdorf, D. J., Arthur, D. C., Brunning, R. & Branda, R. F. (1983). Retinoic acid treatment of acute promyelocytic leukemia: in vitro and in vivo observations. *Blood* **62**(6), 1211-1217.

Fontes, J. D., Kanazawa, S., Jean, D. & Peterlin, B. M. (1999). Interactions between the class II transactivator and CREB binding protein increase transcription of major histocompatibility complex calss II genes. *Molecular and Cellular Biology* **19**, 941-947.

Fumagalli, S., Totty, N. F., Hsuan, J. J. & Courtneidge, S. A. (1994). A target for Src in mitosis. *Nature* **368**(6474), 871-874.

Giacca, A. I. & Kastan, M. B. (1998). The complexity of p53 modulation: emerging patterns from divergent signals. *Genes & Development* **12**, 2973-2983.

Giordano, A. & Avantaggiati, M. L. (1999). p300 and CBP: partners for life and death. *Journal of Cell Physiology* **181**(2), 218-230.

Grande, M. A., van der Kraan, I., de Jong, L. & van Driel, R. (1997). Nuclear distribution of transcription factors in relation to sites of transcription and RNA polymerase II. *Journal of Cell Science* **110**(Pt. 15), 1781-1791.

Grande, M. A., van der Kraan, I., van Steensel, B., Schul, W., de The, H., van der Voort, H. T. H., de Jong, L. & van Driel, R. (1996). PML-containing nuclear bodies: their spatial distribution in relation to other nuclear components. *Journal of Cellular Biochemistry* **63**, 280-291.

Grignani, F., De Matteis, S., Nervi, C., Tomassoni, L., Gelmetti, V., Cioce, M., Fanelli, M., Ruthardt, M., Ferrara, F. F., Zamir, I., Seiser, C., Grignani, F., Lazar, M. A., Minucci, S. & Pelicci, P. G. (1998). Fusion proteins of the retinoic acid receptor-alpha recruit histone deacetylase in promyelocytic leukaemie. *Nature* **391**(6669).

Grignani, F., Fagioli, M., Alcalay, M., Longo, L., Pandolfi, P. P., Donti, E., Biondi, A., Lo Coco, F., Grignani, F. & Pelicci, P. G. (1994). Acute promyelocytic leukemia: from genetics to treatment. *Blood* **83**(1), 10-25.

Grotzinger, T., Sterndorf, T., Jensen, K. & Will, H. (1996). Interferon-modulated expression of genes encoding the nuclear-dot-associated proteins Sp100 and promyelocytic leukemia protein (PML). *European Journal of Biochemistry* **238**, 554-560.

Guldner, H. H., Szostecki, C., Grotzinger, T. & Will, H. (1992). IFN enhance expression of Sp100, an autoantigen in primary biliary cirrhosis. *Journal of Immunology* **149**, 4067-4073.

Hendzel, M. J. & Bazett-Jones, D. P. (1996). Probing nuclear ultrastructure by electron spectroscopic imaging. *Journal of Microscopy* **182**(Pt. 1), 1-14.

Hendzel, M. J., Boisvert, F.-M. & Bazett-Jones, D. P. (1999). Direct visualization of a protein nuclear architecture. *Molecular Biology of the Cell* **10**, 2051-2062.

Hendzel, M. J., Kruhlak, M. J. & Bazett-Jones, D. P. (1998). Organization of highly acetylated chromatin around sites of heterogeneous nuclear RNA accumulation. *Molecular Biology of the Cell* **9**, 2491-2507.

Hodges, M., Tissot, C., Howe, K., Grimwade, D. & Freemont, P. S. (1998). Structure, organization, and dynamics of promyelocytic leukemia protein nuclear bodies. *American Journal of Human Genetics* **63**, 297-304.

Huang, M. E., Ye, Y. C., Chen, S. R., Chai, J. R., Lu, J. X., Zhoa, L., Gu, L. J. & Wang, Z. Y. (1988). Use of all-trans retinoic acid in the treatment of acute promyelocytic leukemia. *Blood* **72**(2), 567-572.

Imhof, A., Yang, X. J., Ogryzko, V. V., Nakatani, Y., Wolffe, A. P. & Ge, H. (1997). Acetylation of general transcription factors by histone acetyltransferases. *Current Biology* **7**(9), 689-692.

Ishidate, T., Yoshihara, S., Kawasaki, Y., Roy, B. C., Toyoshima, K. & Akiyama, T. (1997). Identification of a novel nuclear localization signal in Sam68. *FEBS Letter* **409**(2), 237-241.

Ishov, A. M. & Maul, G. G. (1996). The periphery of nuclear domain 10 (ND10) as site of DNA virus deposition. *Journal of Cell Biology* **134**, 815-826.

Ishov, A. M., Sotnikov, A. G., Negorev, D., Vladimirova, O. V., Neff, N., Kamitani, T., Yeh, E. T., Strauss, J. F. r. & Maul, G. G. (1999). PML is critical for ND10 formation and recruits the PML-interacting protein daxx to this nuclear structure when modified by SUMO-1. *Journal of Cell Biology* **147**(2), 221-234.

Ishov, A. M., Stenberg, R. M. & Maul, G. G. (1997). Human cytomegalovirus immediate early interaction with the host nuclear structures: definition of an immediate transcript environment. *Journal of Cell Biology* **138**, 5-16.

Jackson, D. A. & Cook, P. R. (1985). A general method for preparing chromatin containing intact DNA. *EMBO Journal* **4**(4), 913-918.

Jackson, D. A., Yuan, J. & Cook, P. R. (1988). A gentle method for preparing cyto- and nucleo-skeletons and associated chromatin. *Journal of Cell Science* **90**(Pt. 3), 365-378.

Kakizuka, A., Miller, W. H. J., Umesono, K., Warell, R. P. J., Frankel, S. K., Murty, V. V., Dmitrovsky, E. & Evans, R. M. (1991). Chromosomal translocation t(15;17) in human acute promyelocytic leukemia fuses RAR alpha with a novel putative transcription factor, PML. *Cell* **66**, 663-674.

Kanda, T., Sullivan, K. F. & Wahl, G. M. (1998). Histone-GFP fusion protein enables sensitive analysis of chromosome dynamics in living mammalian cells. *Current Biology* **8**(7), 377-385.

Kastner, P., Perez, A., Lutz, Y., Rochette-Egly, C., Gaub, M. P., Durand, B., Lanotte, M., Berger, R. & Chambon, P. (1992). Structure, localization and transcriptional properties of two classes of retinoic acid receptor alpha fusion proteins in acute promyelocytic leukemia (APL): structural similarities with a new family of oncoproteins. *EMBO Journal* **11**(2), 629-642.

Kitamura, K., Hoshi, S., Koike, M., Kiyoi, H., Saito, H. & Naoe, T. (2000). Histone deacetylase inhibitor but not arsenic trioxide differentiates acute promyelocytic leukaemia cells with t(11;17) in combination with all-trans retinoic acid. *British Journal of Haematology* **108**(4), 696-702.

Kogan, S. C., Hong, S. H., Shultz, D. B., Privalsky, M. L. & Bishop, J. M. (2000). Leukemia initiated by PMLRARalpha: the PML domain plays a critical role while retinoic acid-mediated transactivation is dispensable. *Blood* **95**(5), 1541-1550.

Koken, M. H. M., Linares-Cruz, G., Quignon, F., Viron, A., Chelbi-Alix, M. K., Sobczak-Thepot, J., Juhlin, L., Degos, L., Calvo, F. & de The, H. (1995).

The PML growth-suppressor has an altered expression in human oncogenesis. *Oncogene* **10**, 1315-1324.

Koken, M. H. M., Puvion-Dutilleul, F., Guillemin, M. C., Viron, A., Linares-Cruz, G., Stuurman, N., de Jong, L., Szostecki, C., Calvo, F., Chomienne, C., Degos, L., Puvion, E. & de The, H. (1994). The t(15;17) translocation alters a nuclear body in a retinoic acid-reversible fashion. *EMBO Journal* **13**(1073-1083).

Kretsovali, A., Agalioti, T., Spilianakis, C., Tzortzakaki, E., Merika, M. & Papamatheakis, J. (1998). Involvement of CREB binding protein in expression of major histocompatibility complex class II genes via interaction with the calss II transactivator. *Molecular and Cellular Biology* **18**(6777-6783).

Kruhlak, M. J., Lever, M. A., Fischle, W., Verdin, E., Bazett-Jones, D. P. & Hendzel, M. J. (2000). Reduced Mobility of the Alternate Splicing Factor (ASF) through the Nucleoplasm and Steady State Speckle Compartments. *Journal of Cell Biology* **150**(1), 41-51.

Kwok, R. P., Lundblad, J. R., Chrivia, J. C., Richards, J. P., Bachinger, H. P., Brennan, R. G., Roberts, S. G., Green, M. R. & Goodman, R. H. (1994). Nuclear protein CBP is a coactivator for the transcription factor CREB. *Nature* **370**(6486), 223-226.

Lai, H. K. & Borden, K. L. (2000). The promyelocytic leukemia (PML) protein suppresses cyclin D1 protein production by altering the nuclear cytoplasmic distribution of cyclin D1 mRNA. *Oncogene* **19**(13), 1623-1634.

LaMorte, V. J., Dyck, J. A., Ochs, R. L. & Evans, R. M. (1998). Localization of nascent RNA and CREB binding protein with the PML-containing nuclear

body. *Proceedings of the National Academy of Science of the USA* **95**(4991-4996).

Larghero, J., Zassadowski, F., Rousselot, P. & Padua, R. A. (1999). Alteration of the PML proto-oncogene in leukemic cells does not abrogate expression of MHC class I antigens. *Leukaemia* **13**, 1295-1296.

Lavau, C., Marchio, A., Fagioli, M., Jansen, J., Falini, B., Lebon, P., Grosveld, F., Pandolfi, P. P., Pelicci, P. G. & Dejean, A. (1995). The acute promyelocytic leukaemia-associated PML gene is induced by interferon. *Oncogene* **11**, 871-876.

Le, X. F., Yang, P. & Chang, K. S. (1996). Analysis of the growth and transformation suppressor domains of promyelocytic leukemia gene, PML. *Journal of Biological Chemistry* **271**, 130-135.

Malatesta, M., Zancanaro, C., Martin, T. E., Chan, E. K., Amalric, F., Luhrmann, R., Vogel, P. & Fakan, S. (1994). Is the coiled body involved in nucleolar functions? *Experimental Cell Research* **211**, 415-419.

Manfioletti, G. & Schneider, C. (1988). A new and fast method for preparing high quality lambda DNA suitable for sequencing. *Nucleic Acids Research* **16**(7), 2873-2884.

Marshall, W. F., Fung, J. C. & Sedat, J. W. (1997). Deconstructing the nucleus: global architecture from local interactions. *Current Opinion in Genetics & Development* **7**(2), 259-263.

Martelli, A. M., Cocco, L., Riederer, B. M. & Neri, L. M. (1996). The nuclear matrix: a critical appraisal. *Histology and Histopathology* **11**(4), 1035-1048.

Martinez-Balbas, M. A., Bannister, A. J., Martin, K., Haus-Seuffert, P., Meisterernst, M. & Kouzarides, T. (1998). The acetyltransferase activity of CBP stimulates transcription. *EMBO Journal* **17**(10), 2886-2893.

Mattei, M. G., Petkovich, M., Mattei, J. F., Brand, N. & Chambon, P. (1988). Mapping of the human retinoic acid receptor to the q21 band of chromosome 17. *Human Genetics* **80**, 186-188.

Matunis, M. J., Coutavas, E. & Blobel, G. (1996). A novel ubiquitin-like modification modulates the partitioning of the Ran-GTPase-activating protein RanGAP1 between the cytosol and the nuclear pore complex. *Journal of Cell Biology* **135**(6), 1457-1470.

Maul, G. G. (1998). Nuclear domain 10, the site of DNA virus transcription and replication. *BioEssays* **20**, 660-667.

Maul, G. G., Guldner, H. H. & Spivack, J. G. (1993). Modification of discrete nuclear domains induced by herpes simplex virus type 1 immediate early gene 1 product (ICP0). *Journal of General Virology* **74**(Pt 12), 2679-2690.

Maul, G. G., Ishov, A. M. & Everett, R. D. (1996). Nuclear domain 10 as preexisting potential replication start sites of herpes simplex virus type-1. *Virology* **217**, 67-75.

Misteli, T., Caceres, J. F. & Spector, D. L. (1997). The dynamics of a pre-mRNA splicing factor in living cells. *Nature* **387**(6632), 523-527.

Mu, Z. M., Chin, K. V., Liu, J. H., Lozano, G. & Chang, K. S. (1994). PML, a growth suppressor disrupted in acute promyelocytic leukaemie. *Molecular and Cellular Biology* **14**, 6858-6867.

Muller, S., Matunis, M. J. & Dejean, A. (1998). Conjugation with the ubiquitin-related modifier SUMO-1 regulates the partitioning of PML within the nucleus. *EMBO Journal* **17**, 61-70.

Nagy, L., Kao, H. Y., Chakravarti, D., Lin, R. J., Hassig, C. A., Ayer, D. E., Schreiber, S. L. & Evans, R. M. (1997). Nuclear receptor repression mediated by a complex containing SMRT, mSin3A, and histone deacetylase. *Cell* **89**(3), 373-380.

Nason-Burchenal, K., Gandini, D., Botto, M., Allopenna, J., Seale, J. R. C., Cross, N. P. C., Goldman, J. M., Dmitrovsky, E. & Pandolfi, P. P. (1996). Interferon augments PML and PML/RARa expression in normal myeloid and acute promyelocytic cells and cooperates with all-trans retinoic acid to induce maturation of a retinoid-resistant promyelocytic cell line,. *Blood* **88**, 3926-3936.

Ogryzko, V. V., Schiltz, R. L., Russanova, V., Howard, B. H. & Nakatani, Y. (1996). The transcriptional coactivators p300 and CBP are histone acetyltransferases. *Cell* **87**(5), 953-959.

Okret, S., Carlstedt-Duke, J., Wrange, O., Carlstrom, K. & Gustafsson, J. A. (1981). Characterization of an antiserum against the glucocorticoid receptor. *Biochimica Biophysica Acta* **677**(2), 205-219.

Parkinson, J., Lees-Miller, S. P. & Everett, R. D. (1999). Herpes simplex virus type 1 immediate-early protein vmw110 induces the proteasome-dependent degradation of the catalytic subunit of DNA-dependent protein kinase. *Journal of Virology* **73**(1), 650-657.

Pearson, M., Carbone, R., Sebastiani, C., Cioce, M., Fagioli, M., Shin'ichi, S., Higashimoto, Y., Appella, E., Minucci, S., Pandolfi, P. P. & Pelicci, P. G.

(2000). PML regulates p53 acetylation and premature senescence induced by oncogenic Ras. *Nature* **406**(2), 207-210.

Perez, A., Kastner, P., Sethi, S., Lutz, Y., Reibel, C. & Chambon, P. (1993). PMLRAR homodimers: distinct DNA binding properties and heteromeric interactions with RXR. *EMBO Journal* **12**(8), 3171-3182.

Phair, R. D. & Misteli, T. (2000). High mobility of proteins in the mammalian cell nucleus. *Nature* **404**(6778), 604-609.

Quignon, F., De Bels, F., Koken, M., Feunteun, J., Ameisen, J.-C. & de The, H. (1998). PML induces a novel caspase-independent death process. *Nature Genetics* **20**, 259-265.

Rabl, C. (1885). Uber Zellteilung. *Morphol. Jahrb.* **10**, 214-330.

Raelson, J. V., Nervi, C., Rosenauer, A., Benedetti, L., Monczak, Y., Pearson, M., Pelicci, P. G. & Miller, W. H. J. (1996). The PML/RAR alpha oncoprotein is a direct molecular target of retinoic acid in acute promyelocytic leukemia cells. *Blood* **88**(8), 2826-2832.

Rosenwald, I. B., Kaspar, R., Rousseau, D., Gehrke, L., Leboulch, P., Chen, J. J., Schmidt, E. V., Sonenberg, N. & London, I. M. (1995). Eukaryotic translation initiation factor 4E regulates expression of cyclin D1 at transcriptional and post-transcriptional levels. *Journal of Biological Chemistry* **270**(36), 21176-21180.

Rousseau, D., Kaspar, R., Rosenwald, I., Gehrke, L. & Sonenberg, N. (1996). Translation initiation of ornithine decarboxylase and nucleocytoplasmic transport of cyclin D1 mRNA are increased in cells overexpressing eukaryotic initiation factor 4E. *Proc Natl Acad Sci U S A* **93**(3), 1065-1070.

Rowley, J. D., Golomb, H. M. & Dougherty, C. (1977). 15/17 translocation: a consistent chromosomal change in acute promyelocytic leukemia. *Lancet* **1**, 549-550.

Schardin, M., Cremer, T., Hager, H. D. & Lang, M. (1985). Specific staining of human chromosomes in Chinese hamster x man hybrid cell lines demonstrates interphase chromosome territories. *Human Genetics* **71**(4), 281-287.

Scheer, U. & Weisenberger, D. (1994). The Nucleolus. *Current Opinion in Cell Biology* **6**, 354-359.

Schul, W., de Jong, L. & van Driel, R. (1998). Nuclear neighbours: the spatial and functional organization of genes and nuclear domains. *Journal of Cell Biochemistry* **70**, 159-171.

Schwiebert, L. M., Schleimer, R. P., Radka, S. F. & Ono, S. J. (1995). Modulation of MHC class II expression in human cells by dexamethasone. *Cellular Immunology* **165**, 12-19.

Seksek, O., Biwersi, J. & Verkman, A. S. (1997). Translational diffusion of macromolecule-sized solutes in cytoplasm and nucleus. *Journal of Cell Biology* **138**(1), 131-142.

Shackney, S. E. & Shankey, T. V. (1999). Cell cycle models for molecular biology and molecular oncology: exploring new dimensions. *Cytometry* **35**(2), 97-116.

Shao, W., Fanelli, M., Ferrara, F. F., Riccioni, R., Rosenauer, A., Davison, K., Lamph, W. W., Waxman, S., Pelicci, P. G., Lo Coco, F., Avvisati, G., Testa, U., Peschle, C., Gambacorti-Passerini, C., Nervi, C. & Miller, W. H. J.

(1998). Arsenic trioxide as an inducer of apoptosis and loss of PML/RAR alpha protein in acute promyelocytic leukemia cells. *Journal of the National Cancer Institute* **90**(2), 124-133.

Slack, J. L. & Gallagher, R. E. (1999). The molecular biology of acute promyelocytic leukemia. *Cancer Treatement Research* **99**, 75-124.

Sleeman, J., Lyon, C. E., Platani, M., Kreivi, J. P. & Lamond, A. I. (1998). Dynamic interactions between splicing snRNPs, coiled bodies and nucleoli revealed using snRNP protein fusions to the green fluorescent protein. *Experimental Cell Research* **243**(2), 290-304.

Sleeman, J. E. & Lamond, A. I. (1999). Newly assembled snRNPs associate with coiled bodies before speckles, suggesting a nuclear snRNP maturation pathway. *Current Biology* **9**(19), 1065-1074.

Smith, K. P., Moen, P. T., Wydner, K. L., Coleman, J. R. & Lawrence, J. B. (1999). Processing of endogenous pre-mRNA in association with SC-35 domains is gene specific. *Journal of Cell Biology* **144**, 617-629.

Spector, D. L., Landon, S. & O'Keefe, R. T. (1993). Organization of RNA polymerase II transcription and pre-mRNA splicing within the mammalian cell nucleus. *Biochemistry Society on Transcription* **21**(4), 918-920.

Stadler, M., Chelbi-Alix, M. K., Koken, M. H. M., Venturini, L., Lee, C., Saib, A., Quignon, F., Pelicano, L., Guillemin, M.-C., Schindler, C. & de The, H. (1995). Transcriptional induction of the PML growth suppressor gene by interferons is mediated through an ISRE and a GAS element. *Oncogene* **11**, 2565-2573.

Sterndorf, T., Grotzinger, T., Jensen, K. & Will, H. (1997a). Nuclear Dots: Actors on many stages. *Immunobiology* **198**, 307-331.

Sterndorf, T., Guldner, H. H., Szostecki, T., Grotzinger, T. & Will, H. (1995). Two nuclear-dot associated proteins, PML and Sp100, are often co-autoimmunogenic in patients with primary biliary cirrhosis. *Scandinavian Journal of Immunology* **42**, 257-264.

Sterndorf, T., Jensen, K. & Will, H. (1997b). Evidence for covalent modification of the nuclear dot-associated proteins PML and Sp100 by PIC1/SUMO1. *Journal of Cell Biology* **139**, 1621-1634.

Stuurman, N., de Graaf, A., Floore, A., Josso, A., Humbel, B., de Jong, L. & van Driel, R. (1992). A monoclonal antibody recognizing nuclear matrix-associated nuclear bodies. *Journal of Cell Science* **101**, 773-784.

Szostecki, C., Guldner, H. H., Netter, H. J. & Will, H. (1990). Isolation and characterization of cDNA encoding a human nuclear antigen predominantly recognized by autoantibodies from patients with primary biliary cirrhosis. *Journal of Immunology* **145**, 4338-4347.

Szostecki, C., Krippner, E., Penner, E. & Bautz, F. A. (1987). Autoimmune sera recognize a 100 kD nuclear protein antigen (Sp100). *Clinical Experimental Immunology* **68**, 108-117.

Terris, B. (1995). PML nuclear bodies are general targets for inflammation and cell proliferation. *Cancer Research* **55**, 1590-1597.

Torii, S., Egan, D. A., Evans, R. A. & Reed, J. C. (1999). Human Daxx regulates Fas-induced apoptosis from nuclear PML oncogenic domains (PODs). *EMBO Journal* **18**(21), 6037-6049.

van Steensel, B., Brink, M., van der Meulen, K., van Binnendijk, E. P., Wansink, D. G., de Jong, L., de Kloet, E. R. & van Driel, R. (1995). Localization of the glucocorticoid receptor in discrete clusters in the cell nucleus. *Journal of Cell Science* **108**(Pt. 9), 3003-3011.

Vincent, M., Lauriault, P., Dubois, M. F., Lavoie, S., Bensaude, O. & Chabot, B. (1996). The nuclear matrix protein p255 is a highly phosphorylated form of RNA polymerase II largest subunit which associates with spliceosomes. *Nucleic Acids Research* **24**(23), 4649-4652.

von Mikecz, A., Zhang, S., Montminy, M., Tan, E. M. & Hemmerich, P. (2000). CREB-binding Protein (CBP)/p300 and RNA Polymerase II Colocalize in Transcriptionally Active Domains in the Nucleus. *Journal of Cell Biology* **150**(1), 265-274.

Wang, Z. G., Ruggero, D., Ronchetti, S., Zhong, S., Gaboli, M., Rivi, R. & Pandolfi, P. P. (1998). PML is essential for multiple apoptic pathways. *Nature Genetics* **20**, 266-272.

Wei, X., Somanathan, S., Samarabandy, J. & Berezney, R. (1999). Three-dimensional visualization of transcription sites and their association with splicing factor-rich nuclear speckles. *Journal of Cell Biology* **146**(3), 543-558.

Weis, K., Rambaud, S., Lavau, C., Jansen, J., Carvalgo, T., Carmo-Fonseca, M., Lamond, A. & Dejean, A. (1994). Retinoic acid regulates aberrant nuclear localization of PML-RAR in acute promyelocytic leukemia. *Cell* **76**, 345-356.

Xie, K., Lambie, E. J. & Snyder, M. (1993). Nuclear dot antigens may specify transcriptional domains in the nucleus. *Molecular and Cellular Biology* **13**, 6170-6179.

York, I. A., Goldberg, A. L., Mo, X. Y. & Rock, K. L. (1999). Proteolysis and class I major histocompatibility complex antigen presentation. *Immunology Reviews* **172**, 49-66.

Yoshida, H., Kitamura, K., Tanaka, K., Omura, S., Miyazaki, T., Hachiya, T., Ohno, R. & Naoe, T. (1996). Accelerated degradation of PML-retinoic acid receptor alpha (PML-RARA) oncoprotein by all-trans-retinoic acid in acute promyelocytic leukemia: possible role of the proteasome pathway. *Cancer Research* **56**(13), 2945-2948.

Zheng, P., Guo, Y., Niu, Q., Levy, D. E., Dyck, J. A., Lu, S., Sheiman, L. A. & Liu, Y. (1998). Proto-oncogene PML controls genes devoted to MHC class I antigen presentation. *Nature* **396**, 373-376.

Zhong, S., Hu, P., Ye, T. Z., Stan, R., Ellis, N. A. & Pandolfi, P. P. (1999). A role for PML and the nuclear body in genomic stability. *Oncogene* **18**(56), 7941-7947.

Zhong, S., Salomoni, P. & Pandolfi, P. P. (2000a). The transcriptional role of PML and the nuclear body. *Nature Cell Biology* **2**(5), 85-90.

Zhong, S., Salomoni, P., Ronchetti, S., Guo, A., Ruggero, D. & Pandolfi, P. P. (2000b). Promyelocytic leukemia protein (PML) and Daxx participate in a novel nuclear pathway for apoptosis. *Journal of Experimental Medicine* **191**(4), 631-640.

Zhu, J., Koken, M. H., Quignon, F., Chelbi-Alix, M. K., Degos, L., Wang, Z. Y., Chen, Z. & de The, H. (1997). Arsenic-induced PML targeting onto nuclear bodies: implications for the treatment of acute promyelocytic leukemia. *Proceedings of the National Academy of Science of the USA* **94**(8), 3978-3983.